HHS Public Access

Author manuscript

Dev Biol. Author manuscript; available in PMC 2016 July 31.

Published in final edited form as:

Dev Biol. 2016 July 15; 415(2): 261–277. doi:10.1016/j.ydbio.2016.04.005.

An Fgf-Shh signaling hierarchy regulates early specification of the zebrafish skull

Neil McCarthy[a], **Alfire Sidik**[a], **Julien Y. Bertrand**[c], and **Johann K. Eberhart**[a,b,*]

[a] Department of Molecular Biosciences; Institute of Cell and Molecular Biology, Waggoner Center for Alcohol and Alcohol Addiction Research, University of Texas, Austin, TX, United States [b] Department of Molecular Biosciences; Institute of Neurobiology, University of Texas, Austin, TX, United States [c] Department of Pathology and Immunology, University of Geneva Medical School, Geneva, Switzerland

Abstract

The neurocranium generates most of the craniofacial skeleton and consists of prechordal and postchordal regions. Although development of the prechordal is well studied, little is known of the postchordal region. Here we characterize a signaling hierarchy necessary for postchordal neurocranial development involving Fibroblast growth factor (Fgf) signaling for early specification of mesodermally-derived progenitor cells. The expression of *hyaluron synthetase 2* (*has2*) in the cephalic mesoderm requires Fgf signaling and Has2 function, in turn, is required for postchordal neurocranial development. While Hedgehog (Hh)-deficient embryos also lack a postchordal neurocranium, this appears primarily due to a later defect in chondrocyte differentiation. Inhibitor studies demonstrate that postchordal neurocranial development requires early Fgf and later Hh signaling. Collectively, our results provide a mechanistic understanding of early postchordal neurocranial development and demonstrate a hierarchy of signaling between Fgf and Hh in the development of this structure.

Keywords

Craniofacial development; Head mesoderm; Fgf; Shh; Zebrafish

* Corresponding author at: Department of Molecular Biosciences; Institute of Cell and Molecular Biology, Waggoner Center for Alcohol and Alcohol Addiction Research, University of Texas, Austin, TX, United States. eberhart@austin.utexas.edu (J.K. Eberhart).

Author contributions

Neil McCarthy performed all of the experiments, except those noted below, and helped design all experiments in this manuscript and was the primary author. Alfire Sidik performed *has2* in situ hybridization at 24 hpf and analyzed mesoderm contributions at 48 hpf. Julien Bertrand generated and provided the *drl:CreERT2* transgenic line used for cell fate analysis. Johann Eberhart helped design all experiments and also edited the manuscript, along with Neil McCarthy, Alfire Sidik, and Julien Bertrand.

Appendix A. Supporting information

Supplementary data associated with this article can be found in the online version at http://dx.doi.org/10.1016/j.ydbio.2016.04.005.

No competing interests to disclose.

1. Introduction

The neurocranium is an embryonic structure that generates essential craniofacial structures including the skull vault, skull base, and palate. The palate and skull base are connected and demarcate the prechordal, or anterior, and postchordal, or posterior, regions of the neurocranium, respectively. Extensive fate mapping in tetrapod species demonstrate that the neural crest and mesoderm contribute to the prechordal and postchordal neurocranium, respectively (Couly et al., 1992, 1993; Crump et al., 2004; Eberhart et al., 2006; Gross et al., 2008; Köntges and Lumsden, 1996; McBratney-Owen et al., 2008; Wada et al., 2011). Despite our knowledge of the tissue origins of the neurocranium, mechanistic studies of development have overwhelmingly focused on the prechordal neurocranium, while the postchordal region has been left largely neglected.

For proper formation, the neurocranium requires the orchestration of numerous signaling and morphogenetic events, and is dependent on interactions with surrounding neural as well as non-neural ectoderm, mesoderm, and endoderm (Alexander et al., 2011; Kimmel et al., 2001; Marcucio et al., 2011; Noden and Trainor, 2005; Richtsmeier and Flaherty, 2013). The complexity of these interactions implicates the involvement of multiple signaling molecules in neurocranial development. Much progress has been made in elucidating those factors that induce craniofacial formation and patterning. These factors include many signaling pathways, including Shh, Fgf, Bmp, and Wnt (Alexander et al., 2011; Marcucio, 2005; Richtsmeier et al., 2013; Wada et al., 2005; Wilson and Tucker, 2004). No one single factor can direct craniofacial formation; instead, they interact in spatial and temporal hierarchies that coordinate craniofacial growth and development.

While we know of many of the signaling hierarchies in the neural-crest derived-portions of the craniofacial skeleton, little is known of the mesoderm-derived portions. Hosokawa and colleagues showed that development of the posterior skull vault, a mesoderm-derived structure, involves a signaling hierarchy between TGF-B and Msx2 (Hosokawa et al., 2007). In mouse, chick, and zebrafish, Shh is a critical midline signal necessary for chondrocyte differentiation in the postchordal neurocranium, as well as other regions of the skull (Balczerski et al., 2012a; Eberhart et al., 2006; Wada et al., 2005). Specification of the early cephalic mesoderm, however, is refractory to sonic hedgehog signaling (Balczerski et al., 2012a), suggesting that other signals are necessary for early cephalic mesoderm specification. Due to their proximity to the postchordal neurocranium and their importance in numerous aspects of craniofacial development, the Fibroblast growth factor (Fgf) family is a prime candidate for this function.

Fgfs are part of a large family of intercellular signaling molecules (Itoh, 2007) that emanate from multiple tissue sources in the head. They are also crucial in numerous aspects of craniofacial development, including the proper migration, survival, and patterning of the neural crest (Creuzet et al., 2004; Crump et al., 2006; Hu et al., 2009; Wilson and Tucker, 2004) as well as cranial suture formation (Nie et al., 2006; Rice et al., 2000). Furthermore, Fgfs are implicated in a number of congenital craniofacial disorders with reported skull base defects including Apert and Crouzon syndrome (Aggarwal et al., 2006; Tokumaru et al.,

1996). However, the role that Fgfs play in early postchordal neurocranial development is unknown.

Here, we characterize a signaling hierarchy required for proper postchordal neurocranial development involving Fgf and Shh signaling. Loss of function of both *fgf3* and *fgf8a* lead to a striking loss of the postchordal neurocranium that can be rescued by restoring Fgf3 and Fgf8a signaling centers in the brain and mesoderm. We go on to precisely describe, for the first time, the dual tissue origins of the zebrafish neurocranium. The zebrafish postchordal neurocranium has small pockets of neural crest-derived areas occurring in a mostly mesodermally-derived structure. In situ analysis reveals that both the early cephalic mesoderm marker *hyaluron synthetase 2* (*has2*) and markers for chondrocytes are lost in *fgf3*; *fgf8a* knockdown embryos, and that *has2* is required for postchordal neurocranial development in an Fgf-dependent manner. Examination of Hh loss-of-function embryos reveals that Hh signaling is mostly dispensable for specification of head mesoderm. These results provide evidence of an early signaling interaction required for proper postchordal neurocranial development.

2. Results

2.1. The postchordal neurocranium requires fgf8a and fgf3

The neurocranium can be split into anterior and posterior halves (dashed line in Fig. 1A). While much research has been directed at the development of the neural crest-derived prechordal neurocranium (Fig. 1A, prech.), little is known of the development of the postchordal neurocranium (Fig. 1A, postch.). The postchordal neurocranium includes the parachordal cartilages (pc), which abut the notochord (n); as well as the anterior and posterior basicapsular commissures (abc and pbc, respectively) which encircle the developing ear, the lateral commissures (lc), and the occipital arches (oc) (Fig. 1A; de Beer, 1937). Due to its development adjacent to the notochord and the hindbrain, we reasoned that signals from one or both of these structures could influence posterior neurocranial development.

Fgf8 and Fgf3 signal cooperatively to pattern the hindbrain, making these two Fgfs prime candidates for our analyses. We used a combination of genetic and morpholino-based loss of function of these Fgf ligands, each of which resulted in similar phenotypes (Fig. 1, Supplemental Fig. S1). Whereas neither *fgf8a* nor *fgf3* single-mutants show any profound postchordal neurocranial defects (Fig. 1B and C compared to Fig. 1A), the vast majority of the postchordal neurocranium is absent in double *fgf8a;fgf3* mutants (Fig.1E, arrowhead), with only the prechordal neurocranium and occipital arches remaining. Furthermore, even the loss of a single allele of *fgf3* in an *fgf8a* mutant background gives rise to variable postchordal neurocranial defects, including anterior basicapsular and parachordal cartilage loss (Fig. 1D, arrowheads). These mutants also have severe viscerocranial defects (not shown, Crump et al., 2004). Because, at least, *fgf8a* is maternally expressed (Reifers et al., 1998), we extended our analyses using the well-characterized morpholinos against each of these Fgfs (Crump et al., 2004; Liu et al., 2003; Maves et al., 2002).

Morpholinos targeting either *fgf8a* or *fgf3* injected into *fgf3* or *fgf8a* mutants, respectively, recapitulated postchordal neurocranial defects observed in the double mutants (Supplemental Fig. S1). Embryos injected with *fgf3* morpholinos display infrequent loss of the anterior basicapsular commissure (24%, n=6/24, Supplemental Fig. S1), however the remainder of the neurocranium in these embryos is well developed. Embryos injected with *fgf3* morpholinos also consistently have fused otoliths (Supplemental Fig. S1) as well as variable viscerocranial defects, including fusions of Meckel's cartilage and the palatoquadrate, and loss of the ceratobranchial cartilages (data not shown; Crump et al., 2004). As in our mutant analysis, we found strong synergy between *fgf8a* and *fgf3* in development of the postchordal neurocranium.

In contrast to phenotypes in single mutants, the postchordal neurocranium is lost in *fgf3* morpholino-injected *fgf8a* mutants (100%, n=21/21, Supplemental Fig. S1). The ethmoid plate and trabeculae are retained, albeit reduced, in these embryos (n=21/21). Viscerocranial defects also occur in these embryos, including variable hyosymplectic loss, severe reductions and fusions of Meckel's cartilage and the palatoquadrate (data not shown; Crump et al., 2004). Lastly, we recapitulated the postchordal neurocranial loss in *fgf8a* morpholino-injected *fgf3* mutants (Supplemental Fig. S1). Together, these data show *fgf3* and *fgf8a* synergize during postchordal neurocranial development.

2.2. The mesoderm and neural ectoderm are Fgf sources required for postchordal neurocranium formation

Fgf signaling is required throughout development, forming numerous centers of activity including the mesoderm and neural ectoderm early, and the endoderm and otic placode later (Crump et al., 2004; Sivak et al., 2005; Thisse and Thisse, 2005). To investigate the required Fgf signaling source for postchordal formation, we generated genetic chimeras to re-introduce Fgf signaling from wild-type donor tissues in *fgf3;fgf8* knockdown hosts. We tested four tissue sources: the mesoderm, neural ectoderm, endoderm, and otic placode (Fig. 2, Supplemental Fig. S2). While neither endoderm nor otic placode transplants restored the neurocranium (n=0/12 for endoderm, n=0/9 for otic placode, Fig. 2A–A” and B–B”), we observed a partial rescue of the postchordal neurocranium in embryos receiving either mesoderm or neural ectoderm transplants (n=4/7 for mesoderm, n=8/16 for neural ectoderm, Fig. 2C–C”, D–D” and H). In these transplants most of the parachordal cartilage and anterior basicapsular commissure were present, but rescue was incomplete, suggesting that both tissues might be required. To test this dual requirement, double mesoderm and neural ectoderm transplants were performed, and indeed, complete rescue of the postchordal neurocrania on the transplanted side in *fgf3;fgf8a* loss-of-function hosts was attained (n=4/12 for full rescue, n=3/12 for partial rescue, Figs. 2E–E”, 2H). Together, these data suggest that Fgf signaling from the mesoderm and neural ectoderm cooperate during formation of the postchordal neurocranium.

Fgf signaling from the neural ectoderm induces the otic placode (LÈger and Brand, 2002; Sai and Ladher, 2015). Thus, the partial rescue by neural ectoderm could be indirect, due to a signal relayed from the placode. If this indirect signaling were responsible for the rescue, then loss of the otic placode should phenocopy *fgf8a;fgf3* double loss-of-function embryos.

The otic placode is lost in embryos co-injected, but not singly injected, with *dlx3b* and *foxi1* morpholinos (Solomon et al., 2002, 2003). We found that, as expected, injection of both *dlx3b* and *foxi1* caused complete loss of the otic placode at 24 hpf (Solomon et al., 2004; Supplemental Fig. S3). However, in these embryos only the anterior basicapsular commissure was missing or reduced (Supplemental Fig. S3). In fact, the parachordal cartilages may be expanded. Thus, the otic placode may provide signals regulating postchordal neurocranial development, and future experiments analyzing single versus double loss-of-function embryos would help characterize this role. However, defects to the otic placode itself do not explain the extensive loss of the postchordal neurocranium found in *fgf3;fgf8* loss-of-function embryos.

2.3. The postchordal neurocranium is primarily mesoderm-derived

Deeper analysis of the role of Fgf signaling in postchordal development requires a detailed characterization of the precursors to this structure. However, the origins of the postchordal neurocranium are unknown in zebrafish. To fully characterize any neural crest contribution to the postchordal neurocranium, we utilized three neural-crest labeling transgenic lines, *sox10:KikGR*, *sox10:Kaede*, and *sox10:Cre;ubi:RSG* (Balczerski et al., 2012b; Dougherty et al., 2013; Kague et al., 2012). The *sox10:KikGR* and *sox10:Kaede* embryos were photoconverted at 24 hpf when only neural crest cells express the transgene (Balczerski et al., 2012b; Dougherty et al., 2013), while the *sox10:Cre;ubi:RSG* line genetically labels neural crest cell descendants using a promoter active in neural crest cells (Kague et al., 2012). Results in all 3 lines were identical, with extensive labeling in the ethmoid plate (ep) and trabeculae (tr) of the prechordal neurocranium (Fig. 3A–D and G, data not shown; Eberhart et al., 2006; Kague et al., 2012; Wada et al., 2005). We also observed highly localized labeling within postchordal structures. Labeled areas included the lateral auditory capsule as well as the lateral and anterior-most region of the anterior basicapsular commissure (Figs. 3A-D, 3G). It is of interest that this precise region articulates with the second arch crest-derived hyosympletic of the viscerocranium (Crump et al., 2004).

The first and second arches undergo dynamic morphogenetic movements that involve numerous neural crest-specific cellular rearrangements (Crump et al., 2004, 2006; Eberhart et al., 2006). To elucidate which pharyngeal arch contributes neural crest cells to the postchordal neurocranium, we performed fate mapping with *sox10:Kaede* embryos. We photoconverted either the first or second arch at 26 hpf (Supplemental Fig. S4; Crump et al., 2006), and found that the second arch crest contributed to the lateral auditory capsule (Supplemental Fig. S4), while the first arch crest contributed to the lateral and anterior most region of the anterior basicapsular commissure (Supplemental Fig. S4). Together, these results show that neural crest of the first and second arch contribute to adjacent regions of the postchordal neurocranium.

In both mouse and chicken, mesoderm contributes significantly to the posterior neurocranium. We used the mesoderm-labeling *drl:CreERT2;ubi:switch* line to track mesoderm derivatives in zebrafish (Supplemental Fig. S5; Mosimann et al., 2011). Tamoxifen was added from 6 hpf to 24 hpf to induce Cre- excision. We find a pattern of labeling perfectly complimentary to that generated by the neural crest (Fig. 3E–G). The

parachordal cartilages, posterior basicapsular commissures, and occipital arches appear to be completely of mesoderm origin (Fig. 3E–G). The regions of the anterior basicapsular commissure that were not labeled by neural crest are also of mesoderm origin (Fig. 3E–G). The lateral commissure was the only structure where neural crest and mesoderm cells appear to mix (Fig. 3). Collectively, these data provide a high-resolution fate map of neural crest and mesoderm contribution to the neurocranium and suggest that, even in regions of dual origin, there is little mixing between these cell types.

In order to characterize what happens to this mesoderm population in Fgf loss-of-function embryos, it is necessary to understand their location in the early embryo. We used Kaede photoconversion to label and track groups of cells from 24 hpf to 4 days post-fertilization (dpf), when the postchordal neurocranium is well formed in zebrafish (Fig. 4A–D). We injected *fli1:EGFP* embryos, which labels neural crest early in development but all cartilage later, with *Kaede* mRNA and photoconverted cells just dorsal to the pharyngeal arches for our analyses, a location that should contain mesoderm (Kimmel et al., 1990). In the images, the intense EGFP fluorescence masks the much dimmer green Kaede fluorescence so only the red, photoconverted, Kaede is apparent. We found that at 24 hpf, cells that contribute to the postchordal neurocranium are positioned within the head in relative accord to their location at 4 dpf (Fig. 4E and E', see Supplemental Fig. S6 for individual data). Based on our analyses in Fig. 3 these cells are of mesodermal origin. Overall, no relative change in position of these labeled cells occurred between 24 hpf and 4 dpf. Cells labeled anterior of the otic capsule (o.c.) maintain this position at 4 dpf (Fig. 4E and E', dark gray shade). Those cells labeled more medial and posterior to the otic capsule at 24 hpf populate areas medial and posterior 4 dpf (Fig. 4E and E', gray and light gray shades). During this same time period, neural crest cells appear to undergo extensive cell rearrangements in forming skeletal structures (Crump et al., 2006; Le Pabic et al., 2014). We find little dispersion of labeled mesoderm cells, suggesting a lack of similar rearrangements in the mesoderm-derived skeleton. Together, these data show that the progenitors of the postchordal neurocranium are appropriately positioned along the anterior to posterior axis at 24 hpf.

2.4. Proper specification of the head paraxial mesoderm requires Fgf signaling

Our fate map of the postchordal neurocranium shows that these cartilage precursors are in place by 24 hpf. To investigate whether these precursors are present in embryos lacking *fgf3* and *fgf8a*, we analyzed the expression of the prechondrogenic marker *sox9a* and the cartilage marker *col2a1a*. Compared to un-injected and control morpholino-injected *fgf8a* mutants, *fgf3;fgf8a* double loss-of-function embryos display a loss of *col2a1a* in the cephalic mesoderm (Fig. 5D, compared to A–C, asterisks; Piotrowski and Nusslein-Volhard, 2000). The notochord staining for *col2a1a* is retained in double loss-of-function embryos, demonstrating specificity of the effect (Fig. 5D, arrowheads denote anterior notochord). Furthermore, the pre-cartilage marker *sox9a* is also lost in these *fgf3* morpholino-injected *fgf8a* mutants (Fig. 5H, compared to E–G). Together, these data suggest that the head paraxial mesoderm that will generate these cartilages is either mislocalized or improperly specified when Fgf signaling is attenuated.

To directly address if head paraxial mesoderm is mislocalized in Fgf loss-of-function embryos, we tracked endomesoderm progenitor cells from the initiation of gastrulation (6 hpf) to the end of gastrulation (10 hpf) via Kaede photoconversion. We elaborated on established fate-maps of the mesoderm to label and track postchordal progenitor cells (Kimmel et al., 1990). We injected embryos with Kaede mRNA, photoconverted endomesoderm cells adjacent to the shield at 6 hpf (Fig. 6A-B), and imaged their progression adjacent to the notochord at 10 hpf (Fig. 6C). These labeled cells were then confirmed to contribute to the postchordal neurocranium at 4 dpf (Fig. 6D). Similar to control and Fgf single loss-of-function embryos, mesoderm cells in *fgf3;fgf8a* morpholino-injected embryos migrated to the notochord by 10hpf (Fig. 6H compared to E–G). Furthermore, these cells remain adjacent to the notochord at 24 and 48 hpf (Supplemental Fig. S7). These results demonstrate that head paraxial mesoderm does migrate to its location lateral to the notochord in Fgf loss-of-function embryos and suggest that the postchordal neurocranial defects may be due to a failure in specification of this population of head mesoderm cells.

Because the head paraxial mesoderm expresses *sox9a* and *col2a1a* relatively early in development, we hypothesized that some genes important in chondrocyte maturation would be early markers of this population of head paraxial mesoderm. *Hyaluronan synthetase 2* (*has2*) is required for hyaluronic acid synthesis (Bakkers et al., 2003; Moffatt et al., 2011; Necas et al., 2008; Weigel et al., 1997; Yoshida et al., 2000). Hyaluronic acid is an important extracellular glycosaminoglycan involved in numerous cellular processes including chondrocyte maturation (Moffatt et al., 2011; Necas et al., 2008). Mouse *Has2* knockouts display cephalic mesoderm defects (Camenisch et al., 2000) and in chick limb mesodermal cells, fetal bovine chondrocytes, mouse ear placodal cells, and breast cancer cells, *Has2* is positively regulated by Fgf signaling (Bohrer et al., 2014; Hamerman et al., 1986; Munaim et al., 1991; Urness et al., 2010). These data suggest that *has2* might not only be a marker of head paraxial mesoderm, but may also be involved in the Fgf loss-of-function phenotype.

Our earlier analysis revealed that localization of the head paraxial mesoderm was unperturbed in *fgf3;fgf8* knockdown embryos at 10 hpf. However, by 10 hpf, *has2*-positive cells abutting the notochord in the most anterior region, where the postchordal neurocranium is developing, are lost in *fgf3;fgf8* knockdown embryos (Fig. 7D–D', compared to A–C, A'–C'). Expression of *has2* at 24 hpf is also lost in double *fgf8a; fgf3* mutant embryos (Fig. 7E and F). No gross alterations in earlier *has2* expression, at 6 hpf, could be ascertained in *fgf3;fgf8* knockdown embryos (Supplemental Fig. S8). This suggests that early cephalic mesoderm is not properly specified when Fgf signaling is attenuated.

Chondrocyte maturation has been shown to rely on *has2* function, however, it was unclear whether loss of *has2* contributed directly to the postchordal neurocranial defects in *fgf3;fgf8* knockdown embryos. We injected *fgf8a* mutants with a suboptimal dose of a previously published morpholino targeting *has2* (Bakkers et al., 2004). Wildtype siblings are largely unaffected in the posterior neurocranium (Fig. 7I compared to G), as are control morpholino-injected *fgf8a* mutants (Fig. 7H compared to G). However, *has2* morpholino-injected *fgf8a* mutants display partial loss of the postchordal neurocranium (Fig. 7J, arrowheads). This treatment also causes reductions to the neural crest-derived portion of the

neurocranium, which may be explained by the role of *has2* in the neural crest (Casini et al., 2012). These data suggest that the exacerbated postchordal neurocranial defects observed in *fgf3; fgf8* knockdown embryos is, at least, partially due to loss of *has2*.

The major function of Has2 is in the synthesis of hyaluronic acid (Bakkers et al., 2003; Moffatt et al., 2011; Necas et al., 2008; Weigel et al., 1997; Yoshida et al., 2000), which is known to regulate cartilage development (Matsiko et al., 2012; Matsumoto et al., 2009; Sato et al., 2014). To test the requirement of this function of *has2*, we treated *fgf8a* mutants with a suboptimal concentration of 4-methylumbelliferon (4-MU; Sigma-Aldrich), which is known to inhibit hyaluronic acid production (García-Vilas et al., 2013). Treating *fgf8a* mutants with 4-MU between 6 and 10 hpf did not result in appreciable postchordal neurocranial defects (not shown). However, when treated between 10 and 30 hpf, 4 MU-treated *fgf8a* mutants display loss of *col2a1a* expression at 30 hpf and, at 5 dpf, disruption of mesodermal-derived portions of the postchordal neurocranium, as compared to control-treated *fgf8a* mutants and 4 MU-treated wildtype siblings (Supplemental Fig. S9). Collectively, these data suggest that the postchordal neurocranial defects found in Fgf-compromised embryos is dependent on an early requirement for Fgf signaling on hyaluronic acid production in postchordal neurocranial precursors.

Due to the loss of *has2* expression at 10 hpf in *fgf3;fgf8a* knockdown embryos, we reasoned that Fgf signaling would be required early for postchordal neurocranial development. Using a suboptimal dose of SU5402 (Tocris Biosciences) from 6 to 10 hpf on *fgf8a* mutants and siblings, which only partially reduces Fgf-dependent *etv4* expression at 10 hpf in wildtype and *fgf8a*-treated embryos (Supplemental Fig. S10), we found that, while SU5402-treated wildtypes showed normal neurocranial development (Fig. 8B compared to A and E), both heterozygote and mutant *fgf8a* zebrafish showed postchordal neurocranial defects, affecting the anterior basicapsular commissure in heterozygotes, and the entirety of the postchordal neurocranium in mutants (Fig. 8D compared to A–C and E). Furthermore, *has2* expression at 10 hpf in SU5402-treated *fgf8a* mutants is completely absent in the region of the developing postchordal neurocranium (compare Fig. 8I to F and G). Likewise, at 24 hpf, both *col2a1a* and *sox9a* are reduced in SU5402-treated *fgf8a* mutants (Supplemental Fig. S11). These data strongly suggest that Fgf signaling is required during gastrulation, between 6 and 10 hpf, for postchordal neurocranial formation and specification.

2.5. The notochord is dispensable in the formation of the postchordal neurocranium

Our data show that Fgf signaling, originating from the mesoderm and neural ectoderm, is required in the development of the postchordal neurocranium. Previous reports have shown the importance of Shh signaling from the notochord in this process (Balczerski et al., 2012a). Considering our data, Fgf and Shh together may form a signaling hierarchy required for postchordal neurocranial development. Thus, we investigated the function of the notochord and Shh in the formation of the postchordal neurocranium.

To directly ask whether the maintenance of a notochord is necessary for cephalic mesoderm induction and postchordal neurocranial formation, we analyzed *brachyury* mutants (previously known as no *tail*), which transfate the notochord early in development (Amacher et al., 2002). However, *brachyury* mutants express *has2* at 10 hpf (Fig. 9B–B', compared to

A–A'), *col2a1a* at 24 hpf (Fig. 9D), and retain a postchordal neurocranium (Fig. 9F, compared to E). These data show that notochord maintenance is dispensable for the formation of the postchordal neurocranium.

In *brachyury* mutants, midline sources of Hh remain. To directly test the involvement of Hh signaling in posterior neurocranial development, we analyzed *smo* mutants, which lack all Hh signaling and a postchordal neurocranium (Eberhart et al., 2006). In *smo* mutants, we find that *has 2* expression in the region of the postchordal neurocranium is present (Fig. 10B–B' compared to A–A'), but there are severe reductions in cells expressing the chondrocyte marker *col2a1a* (Fig. 10D compared to C, Eberhart et al., 2006; Wada et al., 2005). Our *smo* data suggests that Hh signaling is required for differentiation of chondrocytes in the mesoderm-derived postchordal neurocranium after 10 hpf.

To directly test the temporal requirement of Hh in the formation of the posterior neurocranium, we utilized the pan-Hh inhibitor cyclopamine (Toronto Research Chemicals; Hirsinger et al., 2004). Treating wild-type embryos from 6 to 10 hpf with cyclopamine did not abolish *has2* expression at 10 hpf in the anterior region of the embryo (Fig. 11B and B' compared to A and A'). In these same embryos, *sox9a* and *col2a1a* expression at 24 hpf remained as well (Fig. 11D and G compared to C and F, respectively), albeit to a potentially lesser degree. However, blocking Hh signaling between 10 and 24 hpf resulted in the complete absence of *sox9a* and *col2a1a* expression (Fig. 11E and H). Together, these data suggest that, while Hh signaling is essential for cartilage differentiation, it plays less of a role in early specification of mesoderm-derived postchordal neurocranial progenitors (Fig. 12). Fgf signaling, on the other hand, is important for this early specification step, via activation of *has 2* (Fig. 12).

3. Discussion

Here we describe a hierarchy of genetic signaling required for the specification and differentiation of the postchordal neurocranium in zebrafish. The postchordal neurocranium is a structure primarily derived from mesoderm, and is lost in embryos with attenuated Fgf or Shh signaling. Fgf signaling plays an early role in the specification of head mesoderm via *has2*. The loss of *has2* and subsequent hyaluronic acid production is at least partly causative of the postchordal neurocranial defects. Shh signaling is then required for the later differentiation of *sox9a* and *col2a1a*-expressing chondrocytes in the postchordal neurocranium. Together, these results reveal a previously unknown genetic signaling hierarchy required in the development of the postchordal neurocranium.

3.1. The dual origin of the zebrafish neurocranium

The zebrafish neurocranium originates from the neural crest and mesoderm. Frog, mouse, and chick fate-maps show similar neurocranial contributions (Couley et al., 1993; Gross and Hanken, 2008; Jiang et al., 2002; Kontges and Lumsden, 1996; McBratney-Owen et al., 2008). Our results strongly suggest that the ancestral pattern of neurocranial contribution is neural crest being largely restricted to prechordal regions, and mesoderm only providing contributions to postchordal regions. The prechordal neurocranium is exclusively of neural-crest origin. This region of the neurocranium has received a good deal of characterization in

zebrafish (Eberhart et al., 2006; Kague et al., 2012; Mongera et al., 2013; Wada et al., 2005), therefore, here we will focus on the postchordal neurocranium.

Using a pan-mesodermal Cre-transgenic line driven by *draculin*, we found that the majority of the postchordal neurocranium is mesoderm-derived. In mouse and chick, the postchordal neurocranium is also primarily mesoderm-derived (Couly et al., 1992, 1993; Kontges and Lumsden, 1996; McBratney-Owen et al., 2008). These data are lacking in frog, however, in neural-crest labeling fate-map studies, non-neural crest derived cartilages are all positioned in the postchordal neurocranium (Gross and Hanken, 2008).

More effort has been spent in mapping the neural crest-derived portions of the prechordal skull (Couly et al., 1993; Gross and Hanken, 2008; Kague et al., 2012; Kontges and Lumsden, 1996; Jiang et al., 2002; McBratney-Owen et al., 2008). Our fate mapping has defined the precise postchordal structures that neural crest cells contribute to in zebrafish, including the most lateral regions of the basicapsular commissures, the lateral auditory capsule, and the parts of the lateral commissures. These areas are important for articulations with the jaw support element the hyosymplectic, as well as muscle attachment sites (Köntges and Lumsden, 1996). Furthermore, first and second arch neural crest cells contribute to distinct regions of the postchordal neurocranium. Along with results in chick (Köntges and Lumsden, 1996), this finding suggests an evolutionarily conserved function of neural crest in forming attachment sites in the postchordal neurocranium with the neural crest-derived jaw, jaw supports, and muscle attachment sites (Köntges and Lumsden, 1996).

3.2. Fibroblast growth factor signaling in the zebrafish neurocranium

The vertebrate neurocranium is the product of the mesoderm and the cranial neural crest, yet requires interactions between multiple tissues. An important regulator of the development of the neural crest-derived portion of the neurocranium is Fibroblast growth factor signaling (Creuzet et al., 2004; Crump et al., 2006; Monsoro-Burq et al., 2003). Our data reveal a second, and much earlier, role for Fgf signaling in the mesoderm-derived postchordal neurocranium.

We show that loss-of-function of both *fgf3* and *fgf8a* cause severe defects in postchordal neurocranial development. The root of this defect is likely the misspecification of cephalic mesoderm at the end of gastrulation. Notably there is a loss of expression of the chondrocyte-regulator *hyaluronan-synthetase 2* (*has2*), which is essential for hyaluronic acid production, positioning *has2* downstream of Fgf. In *fgf8a* mutants, loss of *has2* or hyaluronic acid, led to perturbed postchordal neurocranial defects similar to *fgf3;fgf8* loss-of-function embryos. These data suggest that *has2* is necessary for proper postchordal neurocranial formation in *fgf8a*-dependent fashion. It will be of interest to determine if transgenic activation of *has2* is sufficient to rescue the Fgf loss-of-function defects. How *has2* expression is activated downstream of Fgf signaling and if Fgf signals directly to the head paraxial mesoderm remain to be elucidated. Fgf signaling could maintain *has2* expression directly, via STAT3 activation (Saavalainen et al., 2005). Indeed, Fgf receptors have been shown to activate HAS2 function in breast cancer cells via STAT3 (Bohrer et al., 2014). Understanding the requirement of Fgf receptors in the postchordal neurocranium is of

ongoing interest and will be important to understand the exact mechanism of Fgf-dependent *has2* function in the postchordal neurocranium.

3.3. A signaling hierarchy orchestrates the specification and differentiation of the postchordal neurocranium

Proper craniofacial development relies on complex hierarchies of signaling pathways. Our analysis indicates Fgf signaling from the mesoderm and neuroectoderm is a major regulator of postchordal neurocranial development. Otic placode development is dependent upon signals from the neuroectoderm (LÈger and Brand, 2002; Sai and Ladher, 2015), which could confound our otic placode transplantation results. However, loss of the otic placode itself only results in variable anterior basicapsular commissure loss, not the severe postchordal neurocranial loss phenotype observed in *fgf3;fgf8* knockdown embryos. Thus, the mesoderm and neuroectoderm appear to be the most important sources of Fgf for postchordal development.

Other studies have purported that the notochord is also vital in postchordal neurocranial formation and that *shh* emanating from this structure mediates the formation of the postchordal neurocranium via chondrogenesis of the paraxial mesoderm (Balczerski et al., 2012a). Consistent with this report, we find a loss of differentiated chondrocytes in the postchordal neurocranium. In contrast, *has2* expression was retained, albeit potentially reduced, in *smoothened* mutants, which completely lack Hh signaling (Varga et al., 2001), and in embryos treated with cyclopamine from 6 to 10 hpf compared to controls. This shows that, unlike Fgf signaling, Hh signaling may be dispensable in early specification of postchordal neurocranium precursors, but is certainly important in their terminal differentiation.

The notochord has been thought to be a critical source of Shh for posterior neurocranial development (Balczerski et al., 2012a, 2012b). Analysis of *brachyury* mutants, which transfate the notochord during gastrulation (Amacher et al., 2002; Halpern et al., 1993), showed that the postchordal neurocranium was fully developed and included a chondrocytic region expanded into the area where the notochord develops. The expression of *shh* is maintained in *brachyury* mutants (Amacher et al., 2002). Collectively, these findings suggest that the notochord is not a required *shh* source. However, the possibility remains that, in wild-type embryos, *shh* from the notochord does serve a signaling function to the developing postchordal neurocranium.

Our findings now place Fgf signaling prior to Hh in the formation of the postchordal neurocranium. Cephalic mesoderm is first specified in an Fgf-dependent manner beginning at 10 hpf via activation of *has2*. Temporal-loss of Fgf signaling via SU5402 treatment also shows that Fgf signaling is required early, from 6 to 10 hpf, for *has2* activation. Loss of *has2* ultimately results in the loss of the chondrogenic program resulting in postchordal neurocranial defects in Fgf loss-of-function embryos. Shh, on the other hand, is not essential for this early activation of *has2*, but supports proper chondrogenic differentiation of this group of cells. Together, these results clarify the temporal and genetic control required for proper postchordal neurocranial development in zebrafish.

4. Materials and methods

4.1. Fish husbandry and care

All embryos were raised and cared for using established protocols (Westerfield, 1993) with IACUC approval from the University of Texas at Austin. The *fgf8a*^{ti282a} (Brand et al., 1996), *fgf3*^{24149} (Herzog et al., 2004), *brachyury* ^{b195} (Schulte-Merker et al., 1994), *smoothened*^{b577} (Varga et al., 2001), *sox10:Cre* (Kague et al., 2012), *sox10:KikGR* (Balczerski et al., 2012b), *sox10:kaede* (Dougherty et al., 2013), *ubi:switch* (Mosimann et al., 2011), and *ubi:RSG* (Kikuchi et al., 2010) alleles have all been described previously. The *drl:CreERT2* line was generated using a 3.8 kb *draculin* promoter upstream of the ATG start site. Primers used to amplify this promoter were: for1: ATTGCGGCCGCTTCAATTGTGGTTGAGCAGTC. rev1:ATTACTAGTCCAAGTGTGAATTGGGATCG. The 3.8KB fragment was amplified with iProof polymerase (BioRad), then cloned into TOPO-Blunt (Invitrogen). After verification, the promoter was sub cloned into the Tol2 vector (Kawakami et al., 2004) upstream of the CRE-ERT2 (Feil et al., 1996, PNAS). The Tol2-drl-creert2 vector was co-injected with Tol2 mRNA into AB* in order to establish a founder line. Tamoxifen was added from 10 to 24 h post-fertilization on the *drl:CreERT2* line, and the *sox10:KikGR* and *sox10:kaede* lines were UV-activated at 24 h post-fertilization using DAPI-filter attached to a Zeiss LSM 710. Embryos were treated in embryo media with 5 μM SU5402 (Tocris Biosciences) from 6 to 10 hpf, and 100 μM cyclopamine (Toronto Research Chemicals) or 1 mM 4-methylumbelliferone (Sigma-Aldrich) from 6 to 10 and 10–24 hpf.

4.2. Morpholino and RNA injection

Approximately 5 nl of morpholinos (Gene Tools), working concentrations of 5 mg/ml of a combination of fgf3b and fgf3c morpholinos with sequences 5′GGTCCCATCAAAGAAGTATCATTTG3′ and 5′TCTGCTGGAATAGAAAGAGCTGGC3′, respectively (Maves et al., 2002), of a combination of fgf8aE212 and fgf8aE313 with sequences 5′TAGGATGCTCTTACCATGAACGTCG3′ and 5′CACATACCTTGCCAATCAGTTTCCC3′ (Draper et al., 2001), and control morpholinos with sequence 5′CCTCTTACCTCAGTTACAATTTATA3′ were injected into one- or two-cell stage embryos of *fgf8a* and *fgf3* lines. Approximately 3 nl of a working concentration of 3 mg/ml of *fgfr3* morpholino with sequence 5′AAATGAGGTGTAATGTCTGACCTGT3′ was injected into *fgf8a* mutants. This dose was suboptimal, as it did not cause any defects to wildtype-injected embryos. This is a splice-blocking morpholino targeting the first exon-intron boundary of *fgfr3*. To validate the targeting of this morpholino, whole embryo RNA extracts were isolated from un-injected and *fgfr3* morpholino-injected zebrafish at 24 hpf using Trizol extraction (Invitrogen). cDNA pools were then synthesized using Superscript First-Strand Synthesis System (Invitrogen). To detect changes in mRNA transcripts in morphant embryos, PCR was performed on cDNA pools using the gene-specific primers spanning the morpholino-targeted exon-intron boundary For-TACAGTGCACACCTGCTGTC and revAGCCAATGGATACTGGGCG giving a final size of 491 bp in wildtype. Other morpholinos used that were previously described: dlx3b: 5′-ATATGTCGGTCCACTCATCCTTTAAT-3′ (Solomon et al., 2002); foxi1: 5′-

TAATCCGCTCTCCCTCCAGAAACAT-3′ (Solomon et al., 2003) ; and, *has2*, which required dual injection of two morpholinos: 5′-AGCAGCTCTTTGGAGATGTCCCGTT-3′ and 5′-CGTTAGTTGAACAGGGATGCTGTCC-3′ (Bakkers et al., 2004).

Kaede mRNA was injected into one-cell stage embryos, with or without morpholinos, and UV activated at either 6 or 24 hpf using a Zeiss LSM 710 Confocal microscope.

4.3. Cartilage and bone staining

Five and four day postfertilization (dpf) zebrafish embryos were stained with Alcian blue and Alizarin Red (Walker and Kimmel, 2007), and then were either flat mounted (Kimmel et al., 1998) or had the viscerocrania removed for imaging. Images were taken with a Zeiss Axio Imager-AI microscope. Graphs were made in Microsoft Excel 2011.

4.4. Confocal microscopy and figure processing

Confocal z-stacks were collected on a Zeiss LSM 710 using Zen software. Images were processed in Adobe Photoshop CS. Kaede and tissue fate maps were generated in Adobe Photoshop CS by overlaying images gathered on the Zeiss confocal. Graphs were generated using Microsoft Excel 2011.

4.5. In situ hybridization

RNA in situ hybridization was performed as reported in Miller et al. (2000). AB wildtype, *fgf8a, fgf3;fgf8a* morpholino, *brachyury*, and *smoothened* embryos were treated with 0.0015% PTU (1-phenyl 2-thiourea) to inhibit the production of melanin (Westerfield, 1993). Probes used were *sox9a* (Yan et al., 2002), *col2a1a* (Yan et al., 1995), and the *has2* probe was generated using primers For:ACAAGTCACTGGCCCTATGC and Rev:GGTAGGTAATGGGCGTCTCG (NCBI ref# NM_153650.2). DIC images of in situ hybridizations were collected on a Zeiss Axioimager.

4.6. Cell transplants

Genetic mosaics were generated as described elsewhere (Crump et al., 2004; Maves et al., 2002; Stafford et al., 2006). For neural and otic placode tissue transplants, embryos were injected at the 1-2 cell stage with 2.5% Rhodamine Alexa 568 dextran. At shield stage (6 hpf), donor cells were removed and placed into corresponding areas in *fgf3;fgf8* morpholino-injected hosts using previously described fate maps (Kimmel et al., 1990 and Woo and Fraser, 1995). Mesoderm transplants were performed at shield stage (4 hpf) using donor tissue cells located at the margin and moved to the margins of *fgf3;fgf8* morpholino-injected hosts (Kimmel et al., 1990). For endoderm transplants, donor 1 cell stage embryos were injected with a mixture of 2.5% Rhodamine Alexa 568 dextran and *sox32* mRNA and donor cells located at the margin at shield were transplanted into the margin of *fgf3;fgf8* morpholino-injected hosts (Stafford et al., 2006). For double mesoderm and neural transplants, donor tissue from 2.5% Rhodamine Alexa 568 dextran injected hosts was transplanted at both sphere (taking cells from the margin) and shield (taking cells from the neural ectoderm-forming region) into *fgf3;fgf8* morpholino-injected hosts. At 24 hpf, all hosts were screened using a LeicaM216F fluorescence stereomicroscope for substantial and tissue-specific contributions of donor tissue for subsequent analysis.

Supplementary Material

Refer to Web version on PubMed Central for supplementary material.

Acknowledgments

We wanted to thank the following people for their kind contributions of fish lines, embryos, and morpholinos in this work: Sharon Amacher for the *brachyury* embryos; Gage Crump for the *sox10:Kikgr* line; Sharon Fischer for the *sox10:Cre* line; Eric Liao for the *sox10:Kaede* line; Alex Neichoporuk for the *fgf3* line; and Bruce Riley for the *dlx3b* and *foxi1* morpholinos. We would also like to thank Georgy Koentges, Ben Lovely, Patrick McGurk, Anna Percy, and Mary Swartz for reviewing the manuscript. We would also like to thank Anna Percy for the maintenance and care of all zebrafish lines. This work was supported by NIH/NIDCR grant R01DE020884 and NIH/NIAAA grant U24AA014811 (Riley PI) to JKE; endorsed by a Gabriella Giorgi-Cavaglieri Chair for life sciences and by the Swiss National Fund #31003A_146527 to JYB and NIH/NIAAA F31AA020731 to NM.

References

Aggarwal VS, Liao J, Bondarev A, Schimmang T, Lewandoski M, Locker J, Shanske A, Campione M, Morrow BE. Dissection of Tbx1 and Fgf interactions in mouse models of 22q11DS suggests functional redundancy. Hum. Mol. Genet. 2006; 15(21):3219–3228. [PubMed: 17000704]

Alexander C, Zuniga E, Blitz IL, Wada N, Le Pabic P, Javidan Y, Zhang T, Cho KW, Crump JG, Schilling TF. Combinatorial roles for BMPs and Endothelin 1 in patterning the dorsal-ventral axis of the craniofacial skeleton. Development. 2011; 138(23):5135–5146. [PubMed: 22031543]

Amacher SL, Draper BW, Summers BR, Kimmel CB. The zebrafish T-box genes no tail and spadetail are required for development of trunk and tail mesoderm and medial floor plate. Development. 2002; 129(14):3311–3323. [PubMed: 12091302]

Bakkers J, Kramer C, Pothof J, Quaedvlieg NE, Spaink HP, Hammerschmidt M. Has2 is required upstream of Rac1 to govern dorsal migration of lateral cells during zebrafish gastrulation. Development. 2004; 131(3):525–537. [PubMed: 14729574]

Balczerski B, Matsutani M, Castillo P, Osborne N, Stainier DY, Crump JG. Analysis of sphingosine-1-phosphate signaling mutants reveals endodermal requirements for the growth but not dorsoventral patterning of jaw skeletal precursors. Dev. Biol. 2012b; 362(2):230–241. [PubMed: 22185793]

Balczerski B, Zakaria S, Tucker AS, Borycki AG, Koyama E, Pacifici M, Francis-West P. Distinct spatiotemporal roles of hedgehog signalling during chick and mouse cranial base and axial skeleton development. Dev. Biol. 2012a; 371(2):203–214. [PubMed: 23009899]

de Beer; Gavin. The Development of the Vertebrate Skull. Oxford University Press; Oxford, UK.: 1937.

Bohrer LR, Chuntova P, Bade LK, Beadnell TC, Leon RP, Brady NJ, Ryu Y, Goldberg JE, Schmechel SC, Koopmeiners JS, et al. Activation of the FGFR-STAT3 pathway in breast cancer cells induces a hyaluronan-rich micro-environment that licenses tumor formation. Cancer Res. 2014; 74(1):374–386. [PubMed: 24197137]

Brand M, Heisenberg CP, Jiang YJ, Beuchle D, Lun K, Furutani-Seiki M, Granato M, Haffter P, Hammerschmidt M, Kane DA, et al. Mutations in zebrafish genes affecting the formation of the boundary between midbrain and hindbrain. Development. 1996; 123:179–190. [PubMed: 9007239]

Camenisch TD, Spicer AP, Brehm-Gibson T, Biesterfeldt J, Augustine ML, Calabro A, Kubalak S, Klewer SE, McDonald JA. Disruption of hyaluronan synthase-2 abrogates normal cardiac morphogenesis and hyaluronan-mediated transformation of epithelium to mesenchyme. J. Clin. Investig. 2000; 106(3):349–360. [PubMed: 10930438]

Casini P, Nardi I, Ori M. Hyaluronan is required for cranial neural crest cells migration and craniofacial development. Dev. Dyn. 2012; 241:294–302. [PubMed: 22184056]

Couly GF, Coltey PM, Le Douarin NM. The developmental fate of the cephalic mesoderm in quail-chick chimeras. Development. 1992; 114(1):1–15. [PubMed: 1576952]

Couly GF, Coltey PM, Le Douarin NM. The triple origin of skull in higher vertebrates: a study in quail-chick chimeras. Development. 1993; 117(2):409–429. [PubMed: 8330517]

Creuzet S, Schuler B, Couly G, Le Douarin NM. Reciprocal relationships between Fgf8 and neural crest cells in facial and forebrain development. Proc. Natl. Acad. Sci. USA. 2004; 101(14):4843–4847. [PubMed: 15041748]

Crump JG, Swartz ME, Eberhart JK, Kimmel CB. Moz-dependent Hox expression controls segment-specific fate maps of skeletal precursors in the face. Development. 2006; 133(14):2661–2669. [PubMed: 16774997]

Crump JG, Maves L, Lawson ND, Weinstein BM, Kimmel CB. An essential role for Fgfs in endodermal pouch formation influences later craniofacial skeletal patterning. Development. 2004; 131(22):5703–5716. [PubMed: 15509770]

Dougherty M, Kamel G, Grimaldi M, Gfrerer L, Shubinets V, Ethier R, Hickey G, Cornell RA, Liao EC. Distinct requirements for wnt9a and irf6 in extension and integration mechanisms during zebrafish palate morphogenesis. Development. 2013; 140(1):76–81. [PubMed: 23154410]

Draper BW, Morcos PA, Kimmel CB. Inhibition of zebrafish fgf8 premRNA splicing with morpholino oligos: a quantifiable method for gene knockdown. Genesis. 2001; 30(3):154–156. [PubMed: 11477696]

Eberhart JK, Swartz ME, Crump JG, Kimmel CB. Early Hedgehog signaling from neural to oral epithelium organizes anterior craniofacial development. Development. 2006; 133(6):1069–1077. [PubMed: 16481351]

Feil R, Brocard J, Mascrez B, LeMeur M, Metzger D, Chambon P. Ligand-activated site-specific recombination in mice. Proc. Natl. Acad. Sci. USA. 1996; 93(20):10887–10890. [PubMed: 8855277]

García-Vilas JA, Quesada AR, Medina M. 4-methylumbelliferone inhibits angiogenesis in vitro and in vivo. J. Agric. Food Chem. 2013; 61(17):4063–4071. [PubMed: 23581646]

Gross JB, Hanken J. Segmentation of the vertebrate skull: neural-crest derivation of adult cartilages in the clawed frog, Xenopus laevis. Integr. Comp. Biol. 2008; 48(5):681–696. [PubMed: 21669824]

Halpern ME, Ho RK, Walker C, Kimmel CB. Induction of muscle pioneers and floor plate is distinguished by the zebrafish no tail mutation. Cell. 1993; 75(1):99–111. [PubMed: 8402905]

Hamerman D, Sasse J, Klagsbrun M. A cartilage-derived growth factor enhances hyaluronate synthesis and diminishes sulfated glycosaminoglycan synthesis in chondrocytes. J. Cell. Physiol. 1986; 127(2):317–322. [PubMed: 3754558]

Herzog W, Sonntag C, von der Hardt S, Roehl HH, Varga ZM, Hammerschmidt M. Fgf3 signaling from the ventral diencephalon is required for early specification and subsequent survival of the zebrafish adenohypophysis. Development. 2004; 131(15):3681–3692. [PubMed: 15229178]

Hirsinger E, Stellabotte F, Devoto SH, Westerfield M. Hedgehog signaling is required for commitment but not initial induction of slow muscle precursors. Dev. Biol. 2004; 275(1):143–157. [PubMed: 15464578]

Hosokawa R, Urata M, Han J, Zehnaly A, Bringas P, Nonaka K, Chai Y. TGF-beta mediated Msx2 expression controls occipital somites-derived caudal region of skull development. Dev. Biol. 2007; 310:140–153. [PubMed: 17727833]

Hu D, Marcucio RS. A SHH-responsive signaling center in the forebrain regulates craniofacial morphogenesis via the facial ectoderm. Development. 2009; 136(1):107–116. [PubMed: 19036802]

Itoh N. The Fgf families in humans, mice, and zebrafish: their evolutional processes and roles in development, metabolism, and disease. Biol. Pharm. Bull. 2007; 30(10):1819–1825. [PubMed: 17917244]

Jiang X, Iseki S, Maxson RE, Sucov HM, Morriss-Kay GM. Tissue origins and interactions in the mammalian skull vault. Dev. Biol. 2002; 241(1):106–116. [PubMed: 11784098]

Köntges G, Lumsden A. Rhombencephalic neural crest segmentation is preserved throughout craniofacial ontogeny. Development. 1996; 122(10):3229–3242. [PubMed: 8898235]

Kague E, Gallagher M, Burke S, Parsons M, Franz-Odendaal T, Fisher S. Skeletogenic fate of zebrafish cranial and trunk neural crest. PLoS One. 2012; 7(11):e47394. [PubMed: 23155370]

Kawakami K, Takeda H, Kawakami N, Kobayashi M, Matsuda N, Mishina M. A transposon-mediated gene trap approach identifies developmentally regulated genes in zebrafish. Dev. Cell. 2004; 7(1):133–144. [PubMed: 15239961]

Kikuchi K, Holdway JE, Werdich AA, Anderson RM, Fang Y, Egnaczyk GF, Evans T, Macrae CA, Stainier DY, Poss KD. Primary contribution to zebrafish heart regeneration by gata4(+) cardiomyocytes. Nature. 2010; 464(7288):601–605. [PubMed: 20336144]

Kimmel CB, Warga RM, Schilling TF. Origin and organization of the zebrafish fate map. Development. 1990; 108(4):581–594. [PubMed: 2387237]

Kimmel CB, Miller CT, Moens CB. Specification and morphogenesis of the zebrafish larval head skeleton. Dev. Biol. 2001; 233(2):239–257. [PubMed: 11336493]

Kimmel CB, Miller CT, Kruze G, Ullmann B, BreMiller RA, Larison KD, Snyder HC. The shaping of pharyngeal cartilages during early development of the zebrafish. Dev. Biol. 1998; 203(2):245–263. [PubMed: 9808777]

LÈger S, Brand M. Fgf8 and Fgf3 are required for zebrafish ear placode induction, maintenance and inner ear patterning. Mech. Dev. 2002; 119:91–108. [PubMed: 12385757]

Le Pabic P, Ng C, Schilling TF. Fat-Dachsous signaling coordinates cartilage differentiation and polarity during craniofacial development. PLoS Genet. 2014; 10(10):e1004726. [PubMed: 25340762]

Liu D, Chu H, Maves L, Yan YL, Morcos PA, Postlethwait JH, Westerfield M. Fgf3 and Fgf8 dependent and independent transcription factors are required for otic placode specification. Development. 2003; 130(10):2213–2224. [PubMed: 12668634]

Marcucio RS, Cordero DR, Hu D, Helms JA. Molecular interactions coordinating the development of the forebrain and face. Dev. Biol. 2005; 284(1):48–61. [PubMed: 15979605]

Marcucio RS, Young NM, Hu D, Hallgrimsson B. Mechanisms that underlie co-variation of the brain and face. Genesis. 2011; 49(4):177–189. [PubMed: 21381182]

Matsiko A, Levingstone TJ, O'Brien FJ, Gleeson JP. Addition of hyaluronic acid improves cellular infiltration and promotes early-stage chondrogenesis in a collagen-based scaffold for cartilage tissue engineering. J. Mech. Behav. Biomed. Mater. 2012; 11:41–52. [PubMed: 22658153]

Matsumoto K, Li Y, Jakuba C, Sugiyama Y, Sayo T, Okuno M, Dealy CN, Toole BP, Takeda J, Yamaguchi Y, et al. Conditional inactivation of Has2 reveals a crucial role for hyaluronan in skeletal growth, patterning, chondrocyte maturation and joint formation in the developing limb. Development. 2009; 136(16):2825–2835. [PubMed: 19633173]

Maves L, Jackman W, Kimmel CB. FGF3 and FGF8 mediate a rhombomere 4 signaling activity in the zebrafish hindbrain. Development. 2002; 129(16):3825–3837. [PubMed: 12135921]

McBratney-Owen B, Iseki S, Bamforth SD, Olsen BR, Morriss-Kay GM. Development and tissue origins of the mammalian cranial base. Dev. Biol. 2008; 322(1):121–132. [PubMed: 18680740]

Miller CT, Schilling TF, Lee K, Parker J, Kimmel CB. Sucker encodes a zebrafish Endothelin-1 required for ventral pharyngeal arch development. Development. 2000; 127:3815–3828. [PubMed: 10934026]

Moffatt P, Lee ER, St-Jacques B, Matsumoto K, Yamaguchi Y, Roughley PJ. Hyaluronan production by means of Has2 gene expression in chondrocytes is essential for long bone development. Dev. Dyn. 2011; 240(2):404–412. [PubMed: 21246657]

Mongera A, Singh AP, Levesque MP, Chen YY, Konstantinidis P, Nüsslein-Volhard C. Genetic lineage labeling in zebrafish uncovers novel neural crest contributions to the head, including gill pillar cells. Development. 2013; 140(4):916–925. [PubMed: 23362350]

Monsoro-Burq AH, Fletcher RB, Harland RM. Neural crest induction by paraxial mesoderm in Xenopus embryos requires FGF signals. Development. 2003; 130(14):3111–3124. [PubMed: 12783784]

Mosimann C, Kaufman CK, Li P, Pugach EK, Tamplin OJ, Zon LI. Ubiquitous transgene expression and Cre-based recombination driven by the ubiquitin promoter in zebrafish. Development. 2011; 138(1):169–177. [PubMed: 21138979]

Munaim SI, Klagsbrun M, Toole BP. Hyaluronan-dependent pericellular coats of chick embryo limb mesodermal cells: induction by basic fibroblast growth factor. Dev. Biol. 1991; 143(2):297–302. [PubMed: 1899405]

Necas J, Bartosikova L, Brauner P, Kolar J. Hyaluronic acid (hyaluronan): a review. Vet. Med. 2008; 53

Nie X, Luukko K, Kettunen P. FGF signalling in craniofacial development and developmental disorders. Oral Dis. 2006; 12(2):102–111. [PubMed: 16476029]

Noden DM, Trainor PA. Relations and interactions between cranial mesoderm and neural crest populations. J. Anat. 2005; 207(5):575–601. [PubMed: 16313393]

Piotrowski TN, Nusslein-Volhard C. The endoderm plays an important role in patterning the segmented pharyngeal region in zebrafish (Danio rerio). Dev. Biol. 2000; 225:339–356. [PubMed: 10985854]

Reifers F, Böhli H, Walsh EC, Crossley PH, Stainier DY, Brand M. Fgf8 is mutated in zebrafish acerebellar (ace) mutants and is required for maintenance of midbrain-hindbrain boundary development and somitogenesis. Development. 1998; 125(13):2381–2395. [PubMed: 9609821]

Rice DP, Aberg T, Chan Y, Tang Z, Kettunen PJ, Pakarinen L, Maxson RE, Thesleff I. Integration of FGF and TWIST in calvarial bone and suture development. Development. 2000; 127(9):1845–1855. [PubMed: 10751173]

Richtsmeier JT, Flaherty K. Hand in glove: brain and skull in development and dysmorphogenesis. Acta Neuropathol. 2013; 125(4):469–489. [PubMed: 23525521]

Saavalainen K, Pasonen-Seppänen S, Dunlop TW, Tammi R, Tammi MI, Carlberg C. The human hyaluronan synthase 2 gene is a primary retinoic acid and epidermal growth factor responding gene. J. Biol. Chem. 2005; 280(15):14636–14644. [PubMed: 15722343]

Sai X, Ladher RK. Early steps in inner ear development: induction and morphogenesis of the otic placode. Front. Pharmacol. 2015; 6:19. [PubMed: 25713536]

Sato E, Ando T, Ichikawa J, Okita G, Sato N, Wako M, Ohba T, Ochiai S, Hagino T, Jacobson R, et al. High molecular weight hyaluronic acid increases the differentiation potential of the murine chondrocytic ATDC5 cell line. J. Orthop. Res. 2014; 32:1619–1627. [PubMed: 25196420]

Schulte-Merker S, van Eeden FJ, Halpern ME, Kimmel CB, Nüsslein-Volhard C. no tail (ntl) is the zebrafish homologue of the mouse T (Brachyury) gene. Development. 1994; 120(4):1009–1015. [PubMed: 7600949]

Sivak JM, Petersen LF, Amaya E. FGF signal interpretation is directed by Sprouty and Spred proteins during mesoderm formation. Dev. Cell. 2005; 8(5):689–701. [PubMed: 15866160]

Solomon KS, Fritz A. Concerted action of two dlx paralogs in sensory placode formation. Development. 2002; 129:3127–3136. [PubMed: 12070088]

Solomon KS, Kwak SJ, Fritz A. Genetic interactions underlying otic pla-code induction and formation. Dev. Dyn. 2004; 230:419–433. [PubMed: 15188428]

Solomon KS, Kudoh T, Dawid IB, Fritz A. Zebrafish foxi1 mediates otic placode formation and jaw development. Development. 2003; 130:929–940. [PubMed: 12538519]

Stafford D, White RJ, Kinkel MD, Linville A, Schilling TF, Prince VE. Retinoids signal directly to zebrafish endoderm to specify insulin-expressing beta-cells. Development. 2006; 133(5):949–956. [PubMed: 16452093]

Thisse B, Thisse C. Functions and regulations of fibroblast growth factor signaling during embryonic development. Dev. Biol. 2005; 287(2):390–402. [PubMed: 16216232]

Tokumaru AM, Barkovich AJ, Ciricillo SF, Edwards MS. Skull base and calvarial deformities: association with intracranial changes in craniofacial syndromes. Am. J. Neuroradiol. 1996; 17(4):619–630. [PubMed: 8730180]

Urness LD, Paxton CN, Wang X, Schoenwolf GC, Mansour SL. FGF signaling regulates otic placode induction and refinement by controlling both ectodermal target genes and hindbrain Wnt8a. Dev. Biol. 2010; 340(2):595–604. [PubMed: 20171206]

Varga ZM, Amores A, Lewis KE, Yan YL, Postlethwait JH, Eisen JS, Wester-field M. Zebrafish smoothened functions in ventral neural tube speci-fication and axon tract formation. Development. 2001; 128(18):3497–3509. [PubMed: 11566855]

Wada N, Nohno T, Kuratani S. Dual origins of the prechordal cranium in the chicken embryo. Dev. Biol. 2011; 356(2):529–540. [PubMed: 21693114]

Wada N, Javidan Y, Nelson S, Carney TJ, Kelsh RN, Schilling TF. Hedgehog signaling is required for cranial neural crest morphogenesis and chondrogenesis at the midline in the zebrafish skull. Development. 2005; 132(17):3977–3988. [PubMed: 16049113]

Walker MB, Kimmel CB. A two-color acid-free cartilage and bone stain for zebrafish larvae. Biotech Histochem. 2007; 82:23–28. [PubMed: 17510811]

Weigel PH, Hascall VC, Tammi M. Hyaluronan synthases. J. Biol. Chem. 1997; 272(22):13997–14000. [PubMed: 9206724]

Westerfield, M. The Zebrafish Book: A Guide for the Laboratory use of Zebrafish (Brachydanio rerio). University of Oregon; Eugene, OR.: 1993.

Wilson J, Tucker AS. Fgf and Bmp signals repress the expression of Bapx1 in the mandibular mesenchyme and control the position of the developing jaw joint. Dev. Biol. 2004; 266(1):138–150. [PubMed: 14729484]

Woo K, Fraser SE. Order and coherence in the fate map of the zebrafish nervous system. Development. 1995; 121(8):2595–2609. [PubMed: 7671822]

Yan YL, Hatta K, Riggleman B, Postlethwait JH. Expression of a type II collagen gene in the zebrafish embryonic axis. Dev. Dyn. 1995; 203(3):363–376. [PubMed: 8589433]

Yan YL, Miller CT, Nissen RM, Singer A, Liu D, Kirn A, Draper B, Willoughby J, Morcos PA, Amsterdam A, et al. A zebrafish sox9 gene required for cartilage morphogenesis. Development. 2002; 129(21):5065–5079. [PubMed: 12397114]

Yoshida M, Itano N, Yamada Y, Kimata K. In vitro synthesis of hyaluronan by a single protein derived from mouse HAS1 gene and characterization of amino acid residues essential for the activity. J. Biol. Chem. 2000; 275(1):497–506. [PubMed: 10617644]

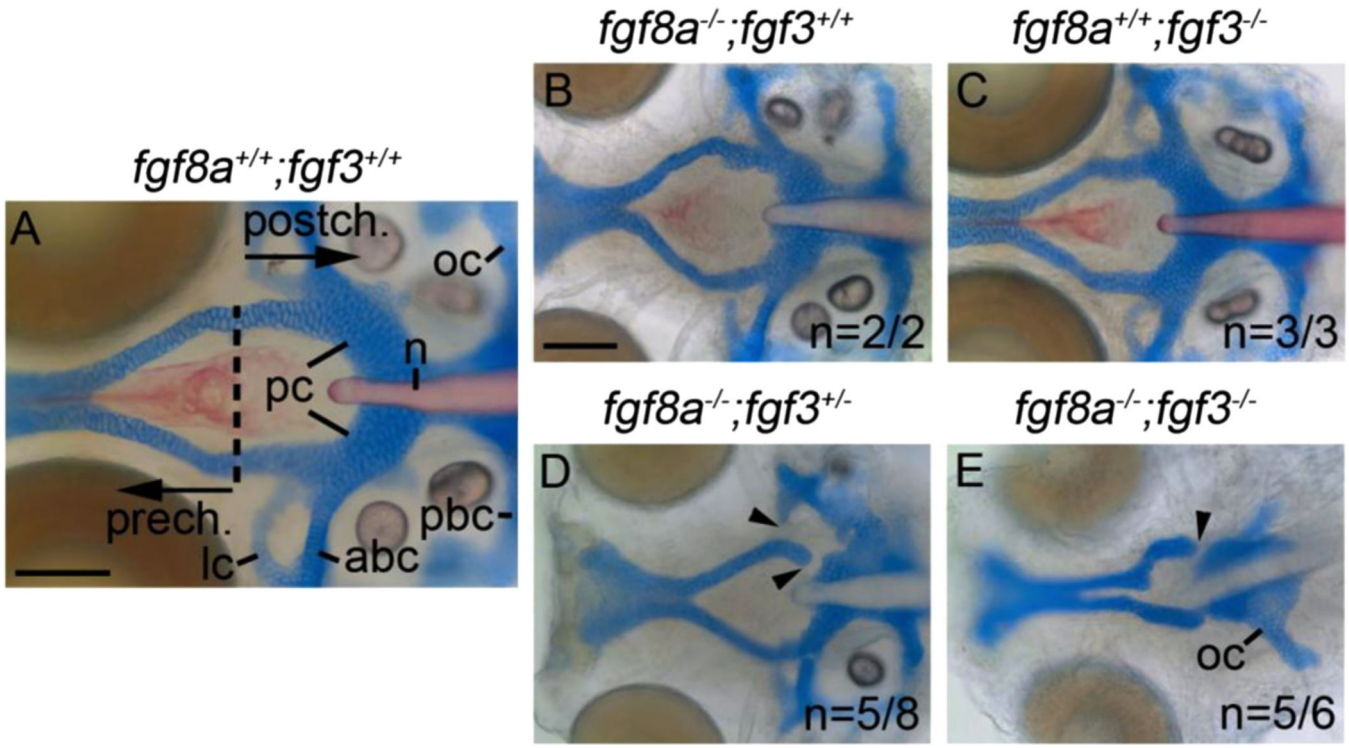

Fig. 1.

The postchordal neurocranium requires Fgf signaling. (A-E) Wholemounted zebrafish neurocrania with the viscerocrania removed at 5 days post-fertilization. Anterior is to the left. (A) Wildtype, showing the prechordal versus postchordal regions of the neurocranium demarcated by a dashed line, (B) *fgf8a* mutant, (C) and *fgf3* mutant embryos display normal neurocrania. (D) Variable neurocranial defects occur in 63% (n=5/8) of $fgf8a^{-/-}$; $fgf3^{+/-}$ embryos (arrowheads). (E) The postchordal neurocranium in $fgf8a^{-/-}$; $fgf3^{-/-}$ embryos is almost completely absent in 83% (n=5/6) of embryos, including the parachordals, anterior and posterior basicapsular commissure and the lateral commissures (arrowhead). abc-anterior basicapsular commissure, lc-lateral commissure, n-notochord, oc-occipital arch, pbc-posterior basicapsular commissure, pc-parachordals, prech.=prechordal neurocranium, postch.=postchordal neurocranium. Scale bar=20 μm.

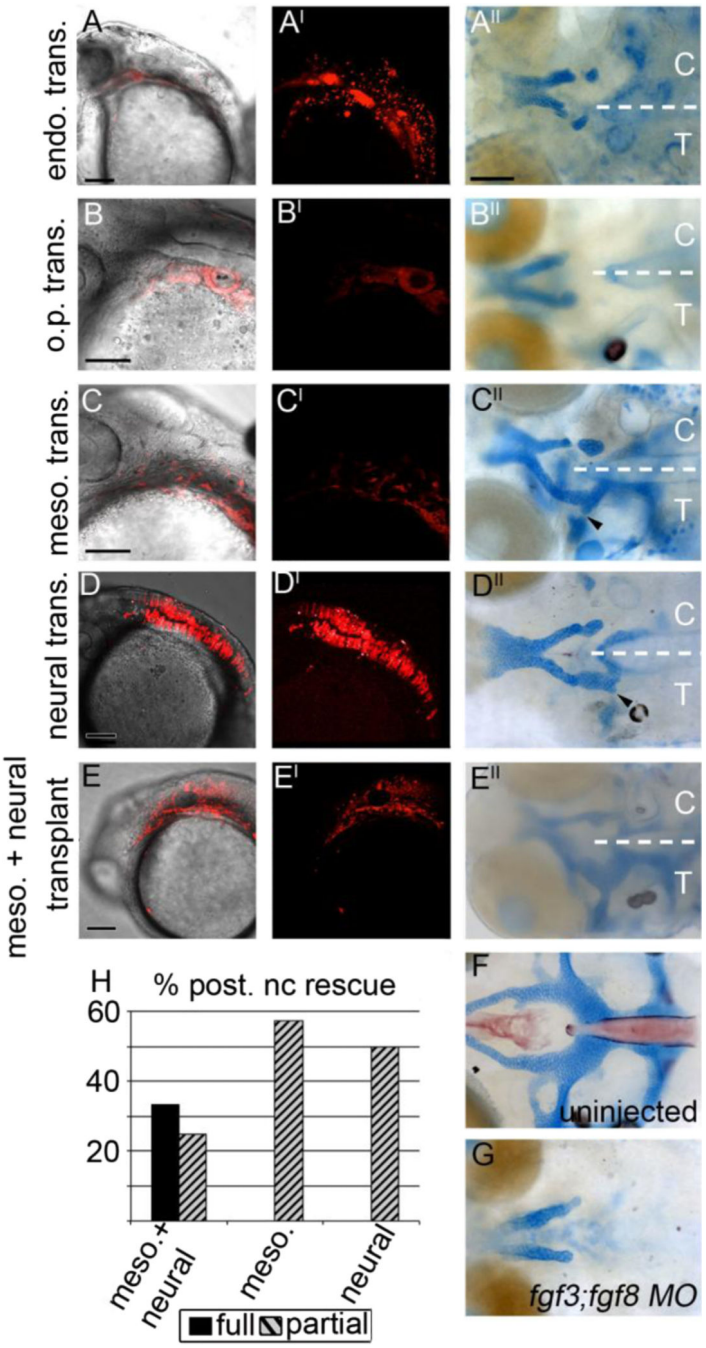

Fig. 2.

The mesoderm and neural ectoderm are Fgf sources required for postchordal neurocranial formation (A–E, A'–E') 24 h post-fertilization confocal images of transplanted wildtype tissues into *fgf3;fgf8* morpholino-injected hosts with and without DIC, respectively; (A"–E") corresponding 4 days post-fertilization (dpf) neurocranial wholemounts with viscerocrania removed. Transplanted side of neurocrania is marked with a T, and control side with a C. (F and G) 4 dpf postchordal neurocrania of uninjected and *fgf3;fgf8* morpholino injected,embryos respectively. Anterior is to the left. (A, A' and A") Endoderm

transplants, (B, B’ and B”) otic placode transplants, (C, C’ and C”) mesoderm only, (D, D’ and D”) neural ectoderm only, and (E, E’ and E”) mesoderm and neural ectoderm double-transplants. Endoderm and otic placode transplants fail to rescue the posterior neurocranium (compare A” and B” to F and G, n=0/12 for endoderm and n=0/9 for otic placode). Transplantation of mesoderm or neural ectoderm alone partially rescues the postchordal neurocranium (compare C” and D” to F and G, n=4/7 for mesoderm and n=8/16 for neural ectoderm). Transplantation of mesoderm and neural ectoderm together can fully rescue the postchordal neurocranium on the side of the embryo receiving the transplant (compare E” to F and G, n=4/12 for full rescue and n=4/12 for partial rescue). Quantification of partial or full rescue is shown in graph H. scale bars=100 μm in A–E and scale bar=20 μm in A”.

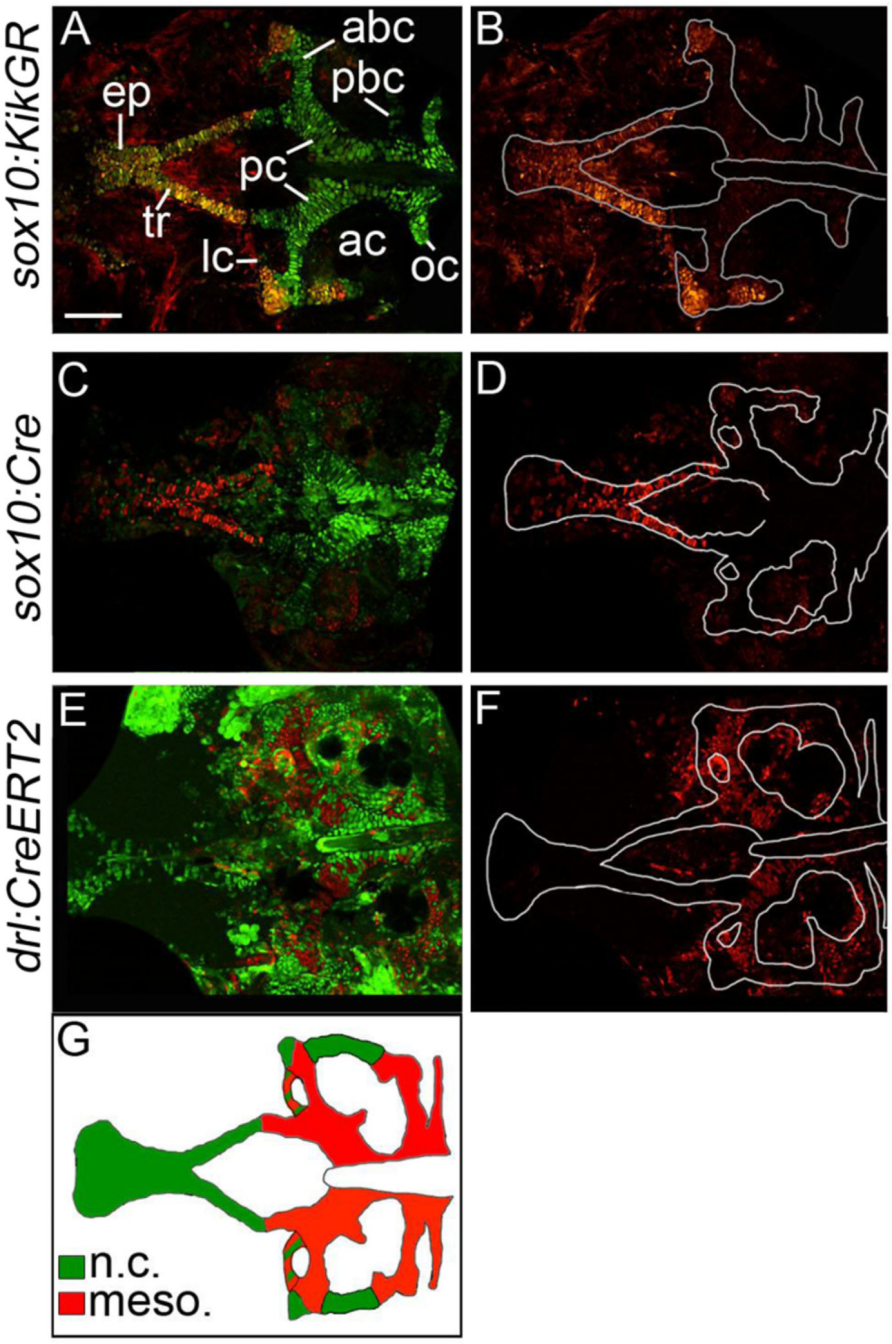

Fig. 3.

The zebrafish postchordal neurocranium is derived from both mesoderm and neural crest tissues. (A–F) Confocal images of 5 days post-fertilization flatmounted zebrafish neurocrania of (A and B) *sox10:KikGR*, (C and D) *sox10:Cre;ubiRSG*, and (E and F) *drl:CreERT2;ubi:switch*. Anterior is to the left. In C and D the red and green channels have been switched for clarity in comparisons to A and B. (B, D and F) Lineage-traced cells only, neurocrania outlined in white. (A–D) Neural crest contributes to the prechordal elements the ethmoid plate and trabeculae, as well as the lateral and anterior regions of the anterior

basicapsular commissures and the lateral auditory capsules. (E and F) Mesoderm contributes the parachordals, anterior and posterior basicapsular commissure, the occipital arch, and the lateral commissures. Schematic of results shown in G ($n \geq 10$ for each transgenic line). abc-anterior basicapsular commissure, ac-auditory capsule, ep-ethmoid plate, lc-lateral commissure, n-notochord, oc-occipital arch, pbc-posterior basicapsular commissure, pc-parachordals, tr-trabeculae. scale bar=50 μm.

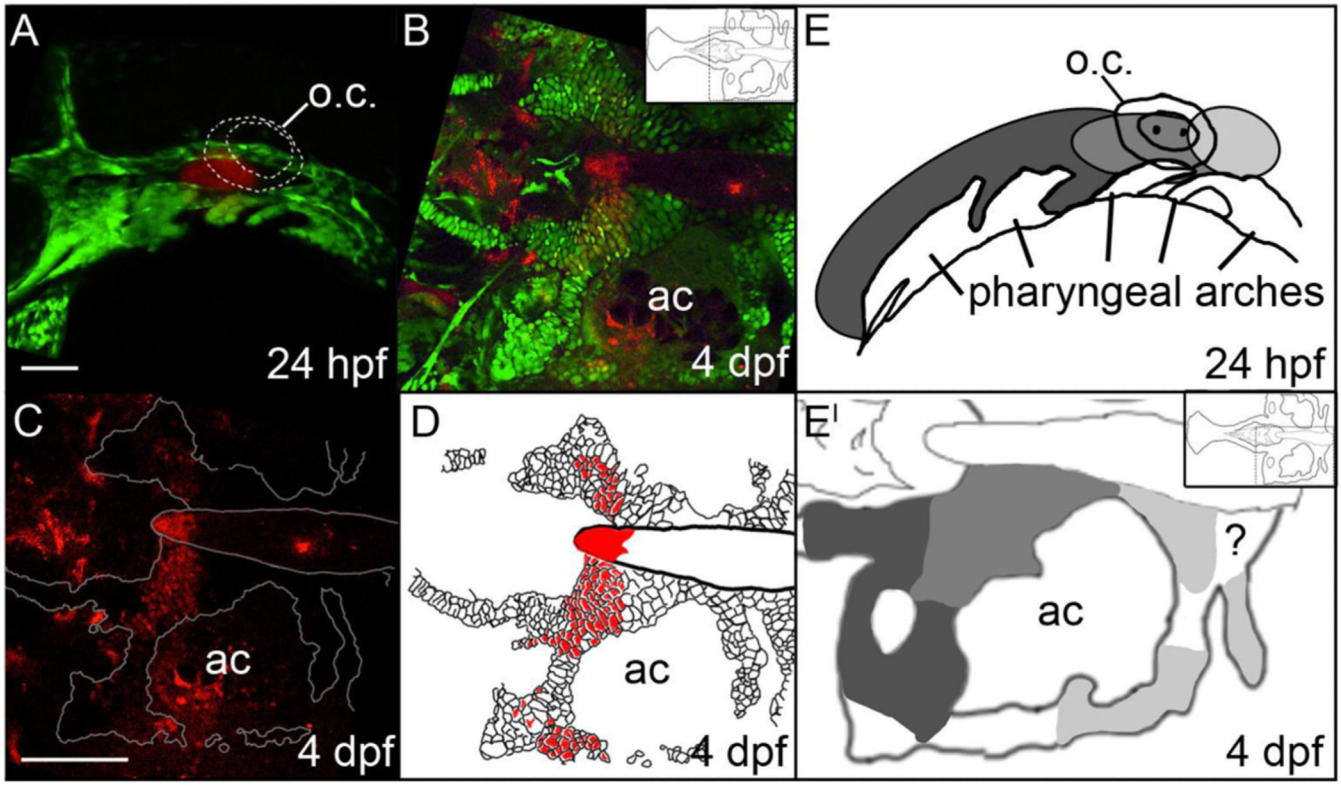

Fig. 4.

The anterior/posterior organization of postchordal cells is set by 24 h post-fertilization (hpf). (A–C) Confocal images of a Kaede-injected embryo at (A) 24 hpf and (B and C) 4 days post fertilization (dpf). Anterior is to the left. (A) At 24 hpf Kaede was photoconverted, shown in red (the remaining green Kaede is not evident due to the intense green fluorescence from the *fli1:EGFP* transgene), and (B) at 4 dpf, this same embryo shows labeling in the postchordal neurocranium (inset shows relative position in the neurocranium of magnified view). (C) Red channel only, the neurocrania is outlined in white. (D) Schematic of panel C, with red cells depicting the photoconverted region. (E and E') Graphical representation of Kaede-mediated fate mapping at 24 hpf and 4 dpf. Inset in E' shows relative position of magnified neurocrania. Question mark denotes a region that remained unlabeled in our analyses. ac-auditory capsule, o.c.-otic capsule. Scale bars=10 μm in A and 20 μm in C.

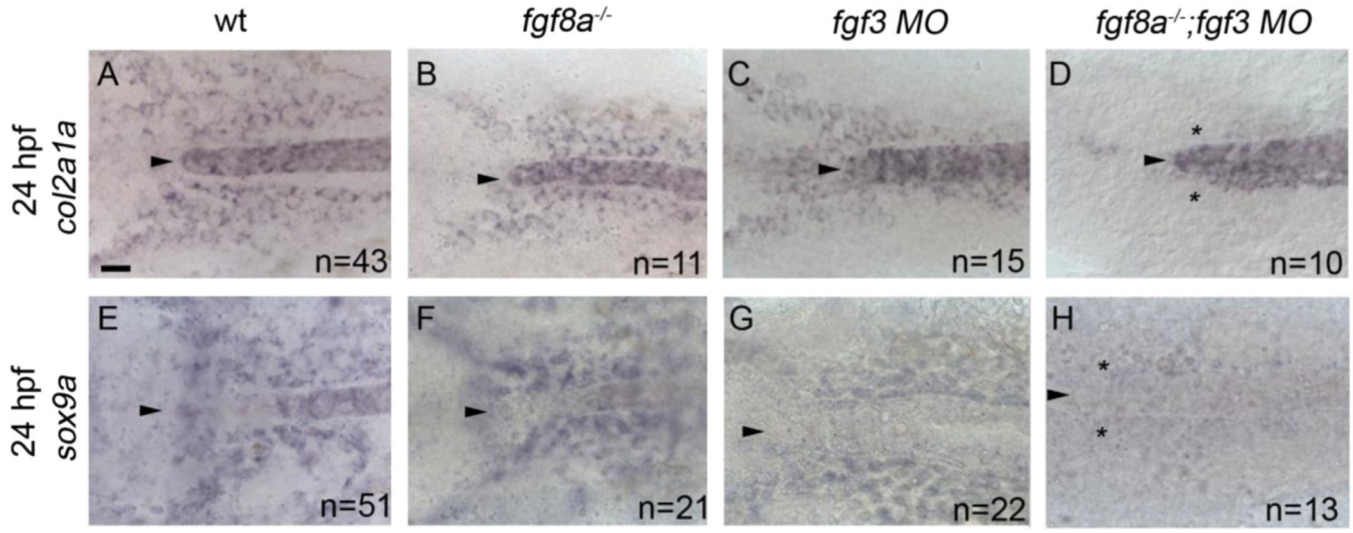

Fig. 5.

Cartilage and pre-cartilage markers *col2a1a* and *sox9a* are absent at 24 h post-fertilization (hpf) in *fgf3;fgf8a* knockdown embryos. (A–H) Images of 24 hpf embryos labeled with (A–D) *col2a1a* and (E–H) *sox9a* riboprobe. Dorsal view with anterior to the left, arrowhead denotes the anterior limit of the notochord. (A and E) Wildtype, (B and F) *fgf8a* mutant, and (C and G) *fgf3* morpholino embryos display normal expression of both *col2a1a* and *sox9a*. However, (D and H) *fgf3* morpholino-injected *fgf8a* mutants lose the expression of both *col2a1a* and *sox9a* (asterisk). scale bar=20 μm.

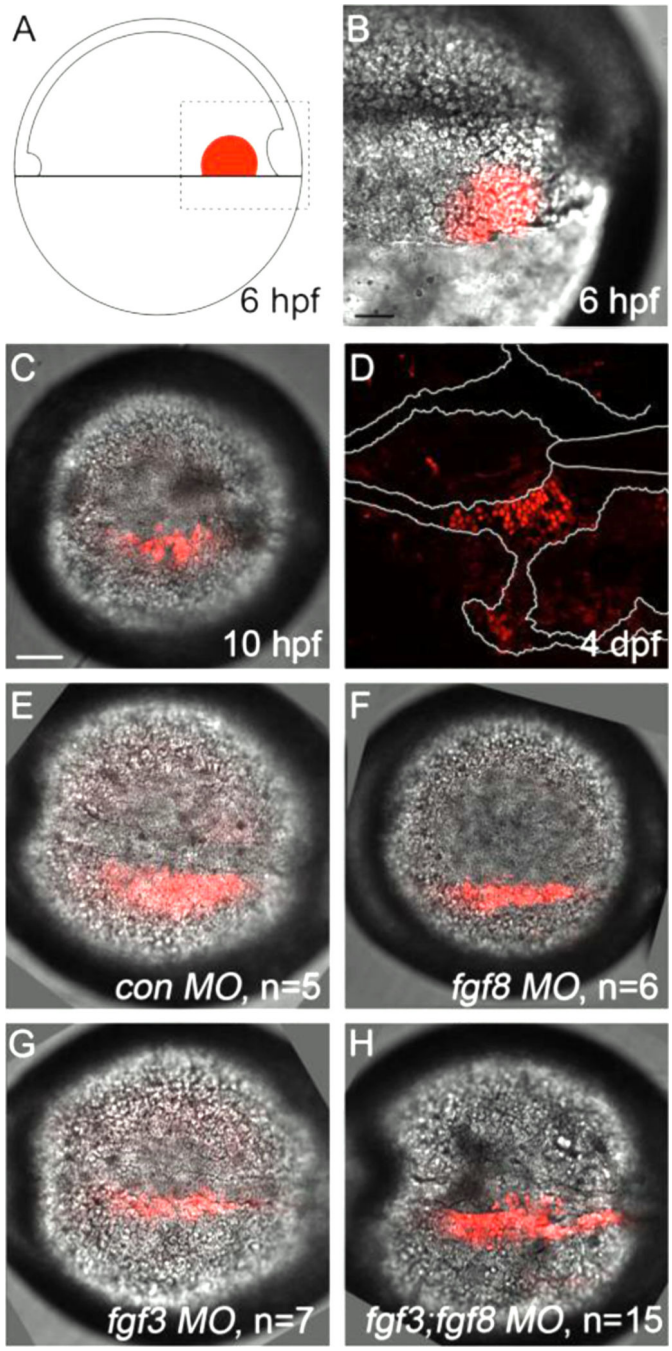

Fig. 6.

Kaede photoconverted endomesoderm postchordal-progenitor cells migrate appropriately in *fgf3;fgf8a* knockdown embryos. (A) Schematic of 6 h post-fertilization (hpf) zebrafish embryo showing the region of the embryo photoconverted in all subsequent experiments, dorsal to the right. (B–D) DIC confocal images showing the photoconverted area at 6 hpf (B, magnified region outlined in A), 10 hpf (C), and 4 days post-fertilization (dpf) (D). Cells have migrated adjacent to the notochord by 10 hpf and contributed to the postchordal neurocranium at 4 dpf. At 10 hpf, cells in (E) control, (F) *fgf8*, (G) *fgf3*, and (H) *fgf3;fgf8*

double morpholino-injected embryos are appropriately positioned (compared to C). scale bar=20 μm.

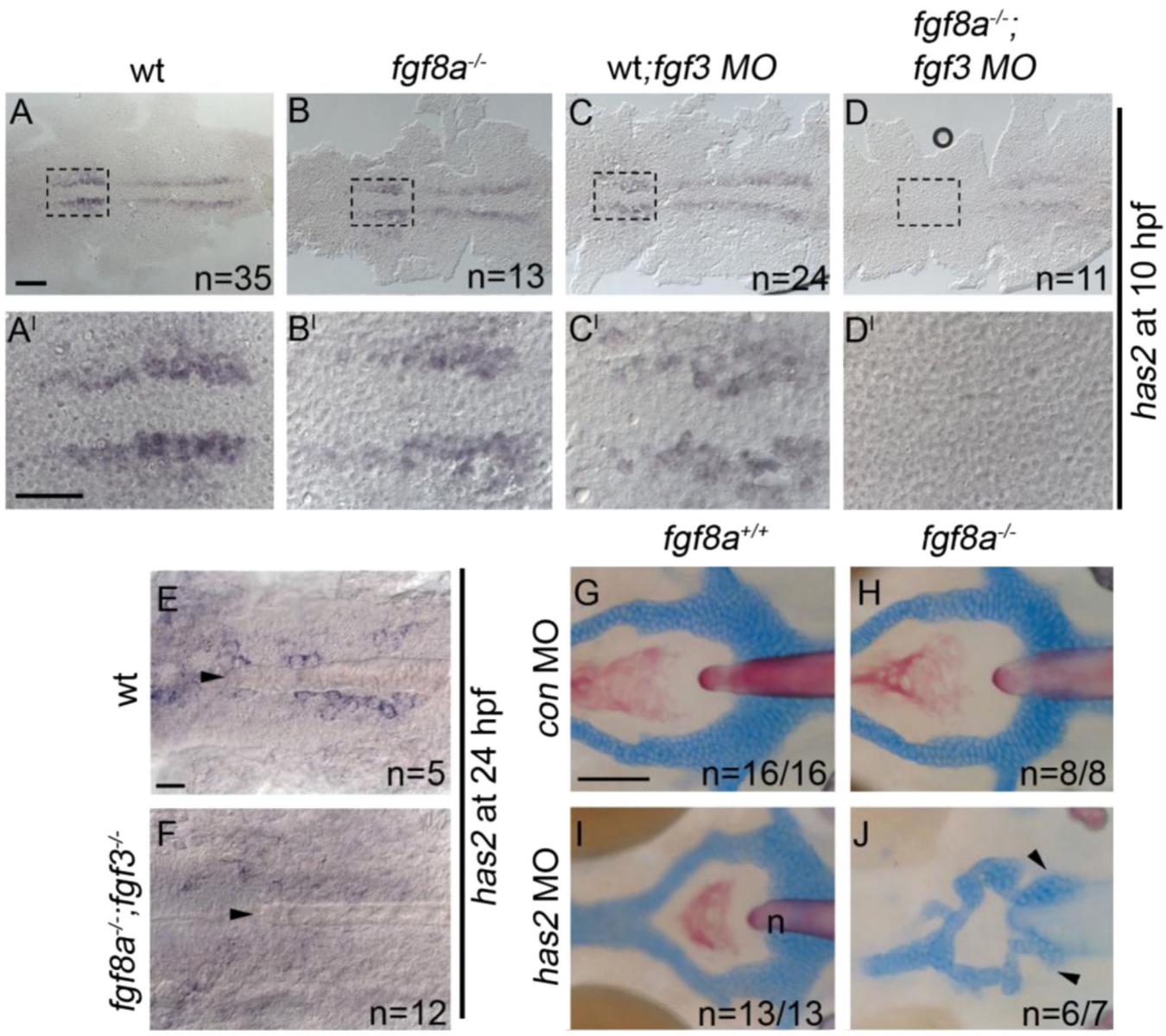

Fig. 7.

Loss of *has2* in Fgf knockdown embryos contributes to the postchordal neurocranial loss phenotype. (A–D, A'–D') Images of 10 h post-fertilization, and (E–F) 24 h post-fertilization embryos labeled with *has2* riboprobe. Dorsal view and anterior to the left in all images. (G–J) Wholemounted zebrafish neurocrania with the viscerocrania removed at 5 days post fertilization. Anterior is to the left. (A'–D') Magnified areas of region outlined in (A–D). (A and A') Uninjected wildtype, (B and B') *fgf8a* mutants, and (C and C') *fgf3* morpholino-injected wildtype display normal expression of *has2*, however, (D and D') *fgf3* morpholino-injected *fgf8a* mutants exhibit loss of expression of *has2* in the presumptive postchordal neurocrania (D and D'). (E) At 24 hpf, some *has2* expression remains along the notochord, however, (F) expression is lost in *fgf8a;fgf3* double mutant embryos. Arrowheads denote end of the notochord. (G) Control morpholino-injected wildtype and (H) *fgf8a* mutants, as well

as (I) *has2* morpholino-injected wildtypes retain the postchordal neurocranium. However, (J) *has2* morpholino-injected *fgf8a* mutants have a substantial loss of the postchordal neurocranium (arrowheads). n=notochord. scale bar=50 μm in A, 10 μm in A' and E, and 20 μm in G.

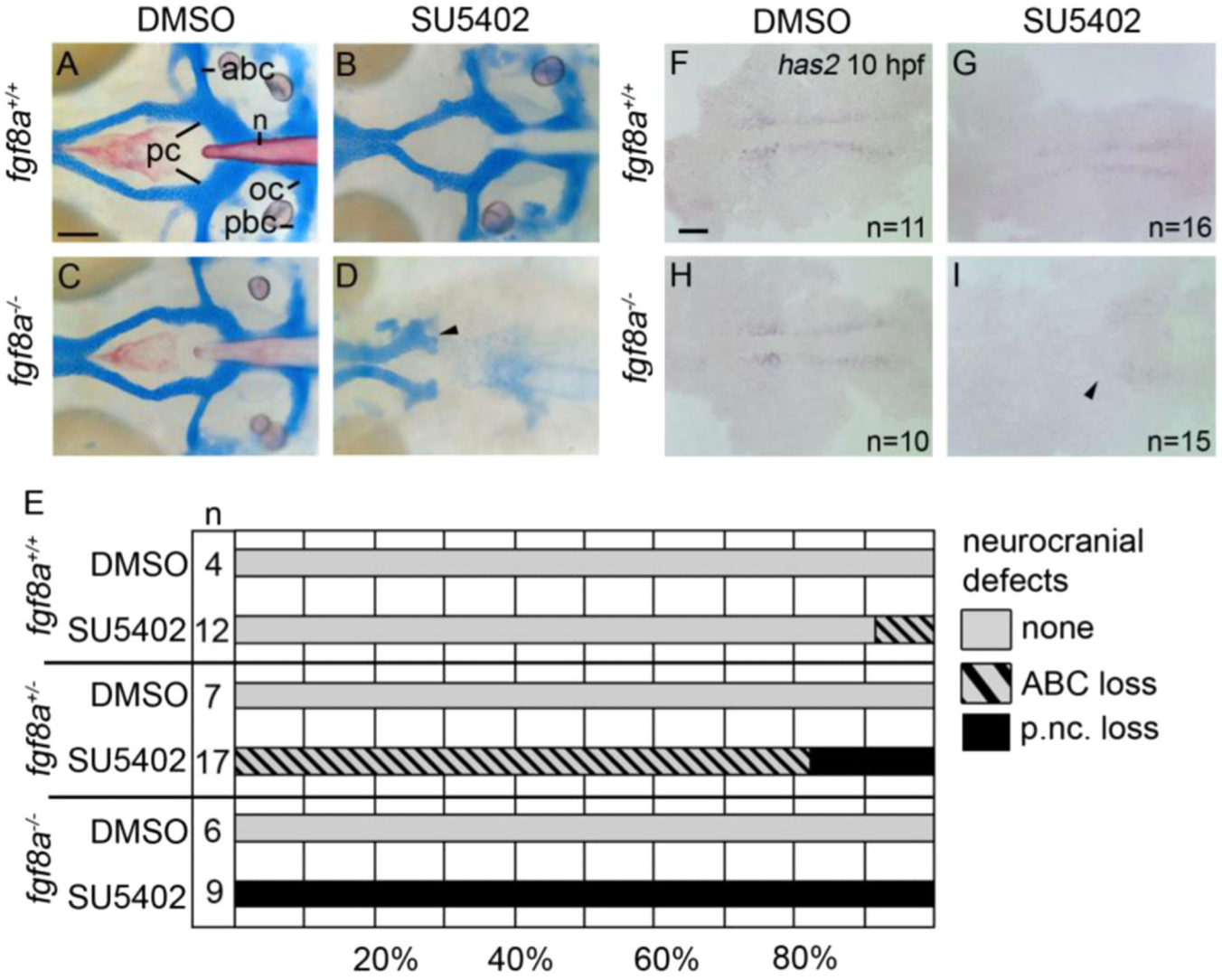

Fig. 8.

Postchordal neurocranial development requires Fgf signaling during gastrulation. (A–D) Wholemount zebrafish neurocrania, anterior is to the left. (A and B) Wildtype neurocrania treated with DMSO or SU5402 develop normally. (C) DMSO-treated *fgf8a* mutants are also unaffected, however, (D) those treated with SU5402 from 6 to 10 hpf develop severe postchordal neurocranial loss. (E) Quantification of postchordal neurocranial defects including none (see A), ABC loss, or complete postchordal neurocranial loss (p. nc. loss) in DMSO and SU5402 treated wildtype (*fgf8a*+/+), heterozygous (*fgf8a*+/−) and mutant (*fgf8a* −/−) embryos. (F–H) DMSO-treated wildtype and *fgf8a* mutants and SU5402-treated wildtype express *has2* appropriately; however, (I) SU5402-treated *fgf8a* mutants display a loss of expression of *has2* in postchordal neurocranial precursors (arrowhead denotes most anterior expression). abc- anterior basicapsular commissure, lc-lateral commissure, n-notochord, oc-occipital arch, pc-parachordals, pbc-posterior basicapsular commissure. scale bar=20 μm in A and scale 10 μm in F.

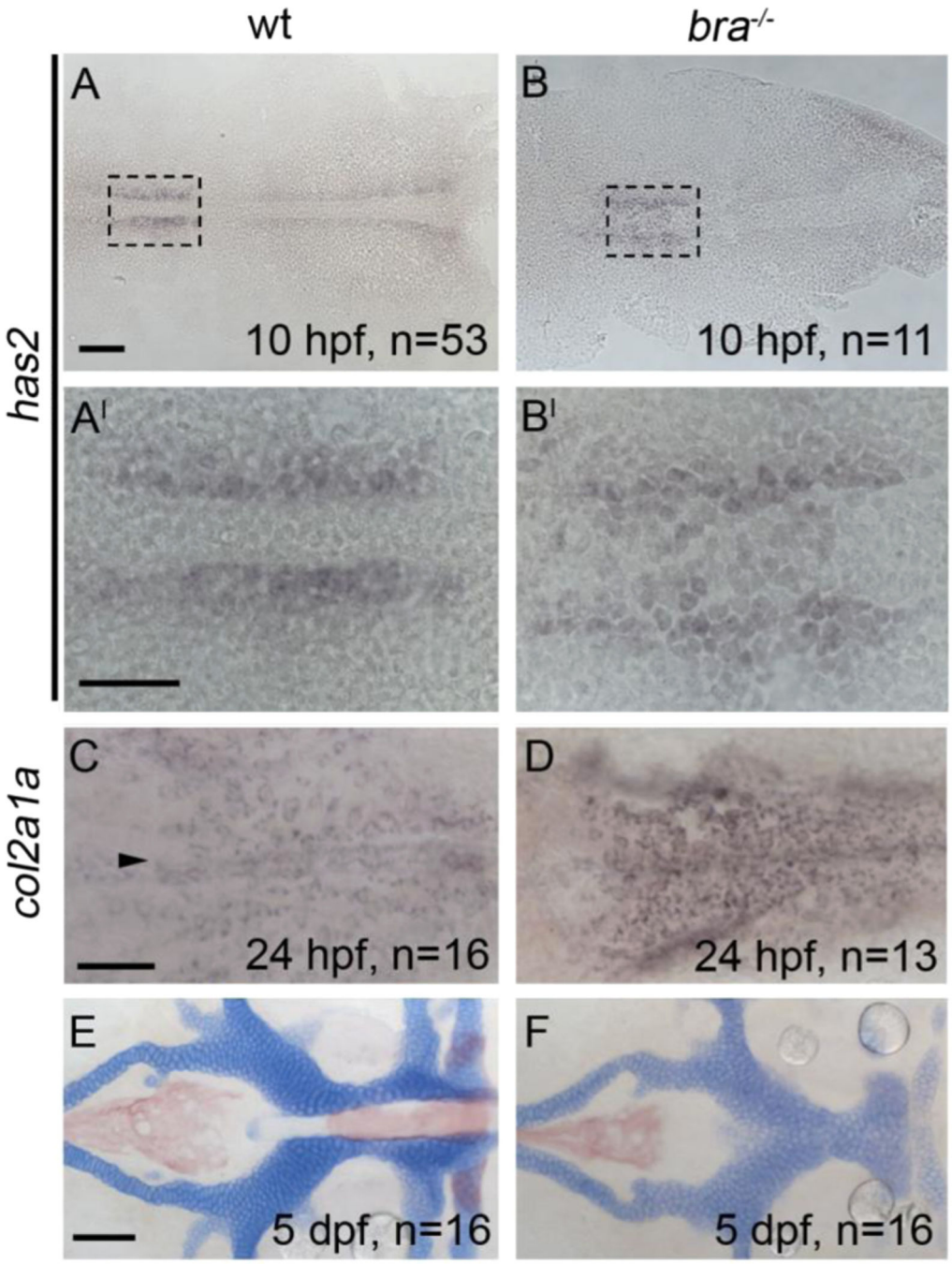

Fig. 9.

Postchordal neurocranial development does not require *brachury* function or a notochord. Anterior is to the left in all panels. (A–B, A'–B') *hyaluronan synthetase 2* (*has2*) is expressed in cephalic regions at 10 h post-fertilization (hpf) in both wildtypes and *brachury* mutants. (C and D) The late chondrogenic marker *col2a1a* at 24 hpf appears in both *brachury* mutants and siblings in the forming postchordal area of the developing embryo (compare D to C, arrowhead in C denotes anterior notochord). (E and F) At 5 days post-fertilization, postchordal neurocrania of *brachury* mutants are normal, *sans* notochord,

compared to siblings (compare F to E). scale bar=50 μm in A and 10 μm in A’ and C and 20 μm in E.

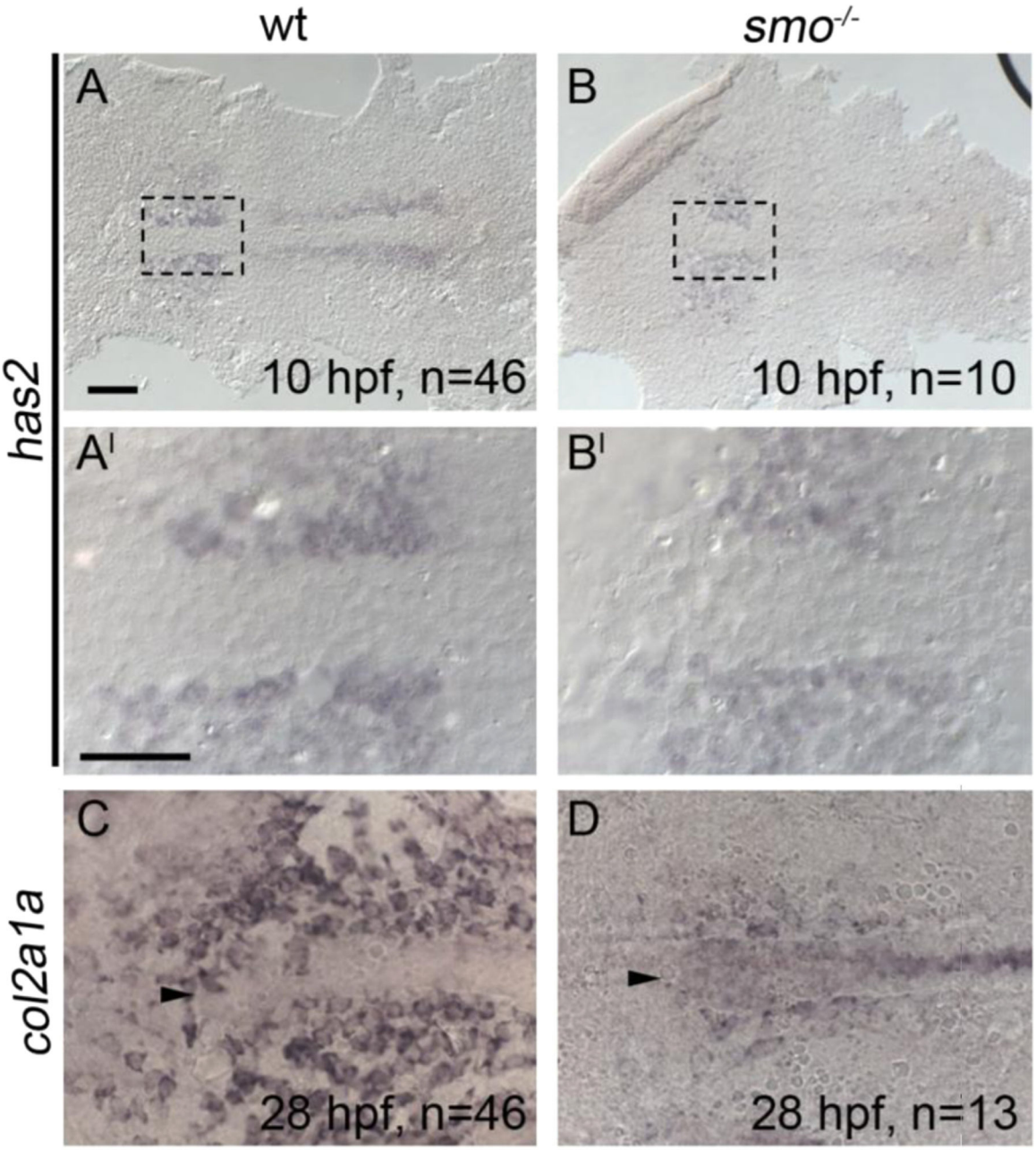

Fig. 10.

Chondrocyte differentiation is particularly sensitive to disruption of Hh signaling. All panels are anterior to the left. (A–B, A'–B') At 10 h post-fertilization (hpf), the early mesoderm marker *has2* is expressed in the anterior region of *smoothened* mutants and wildtypes (Compare B to A, B' to A'). (C and D) However, *smoothened* mutants display a marked reduction in *col2a1a* expression in the forming postchordal neurocranium at 28 hpf compared to siblings (compare D to C, arrowhead denotes anterior notochord). Scale bar=50 μm in A and 10 μm in A'.

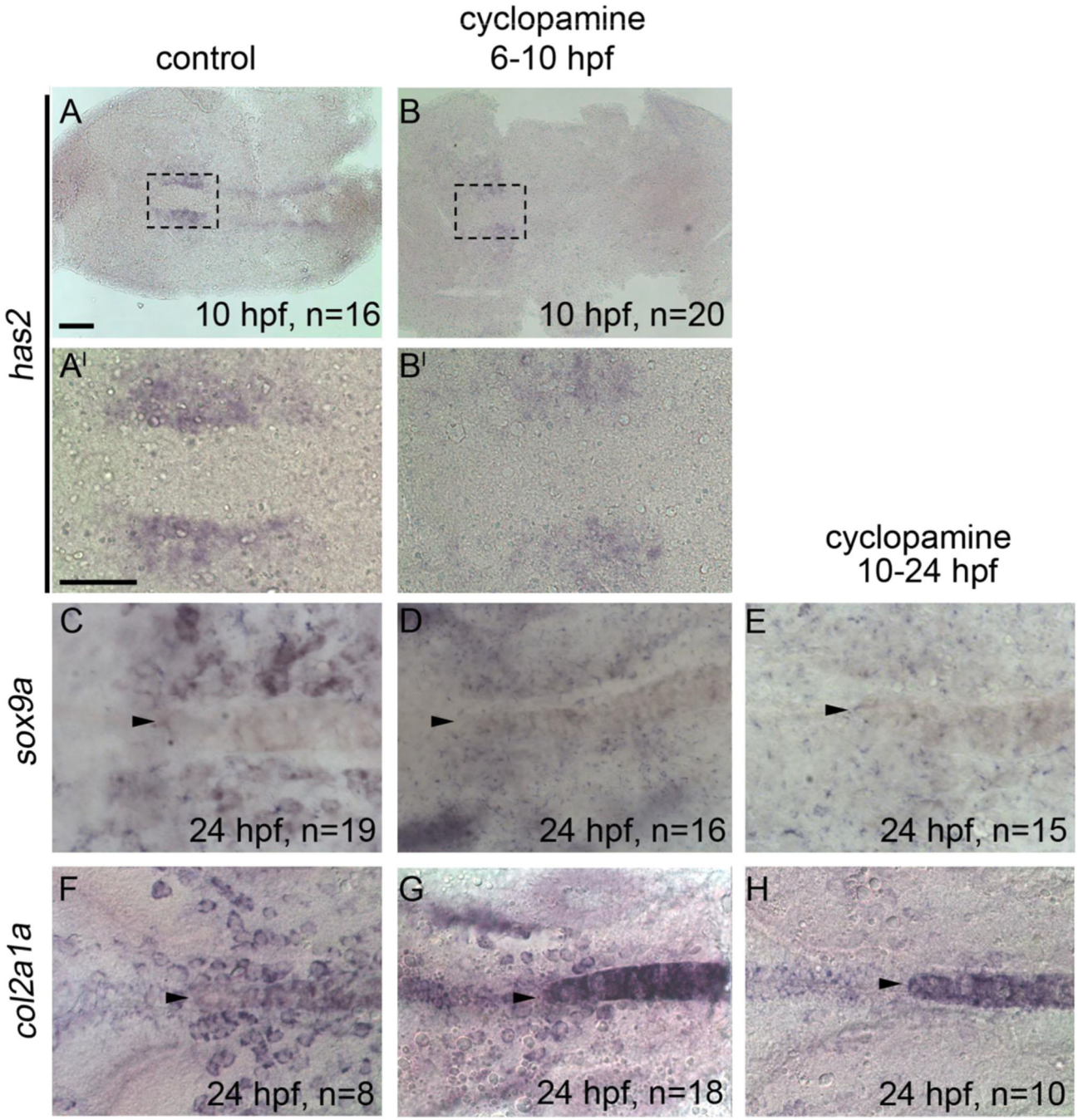

Fig. 11.

Hh signaling is required after Fgf signaling for postchordal neurocranial development. The expression of *has2* is retained following either (A–A') DMSO or (B–B') cyclopamine treatment from 6 to 10 h post-fertilization (hpf). (C and D and F–H) DMSO- and cyclopamine-treated embryos from 6 to 10 hpf show expression of both *sox9a* and *col2a1a* at 24 hpf, however, (*E* and H) cyclopamine-treated embryos from 10 to 24 hpf show a loss of *sox9a* and *col2a1a* expression in the postchordal neurocranium at 24 hpf. Arrowheads denote the anterior limit of the notochord. scale bar=50 μm in A and 10 μm in A'.

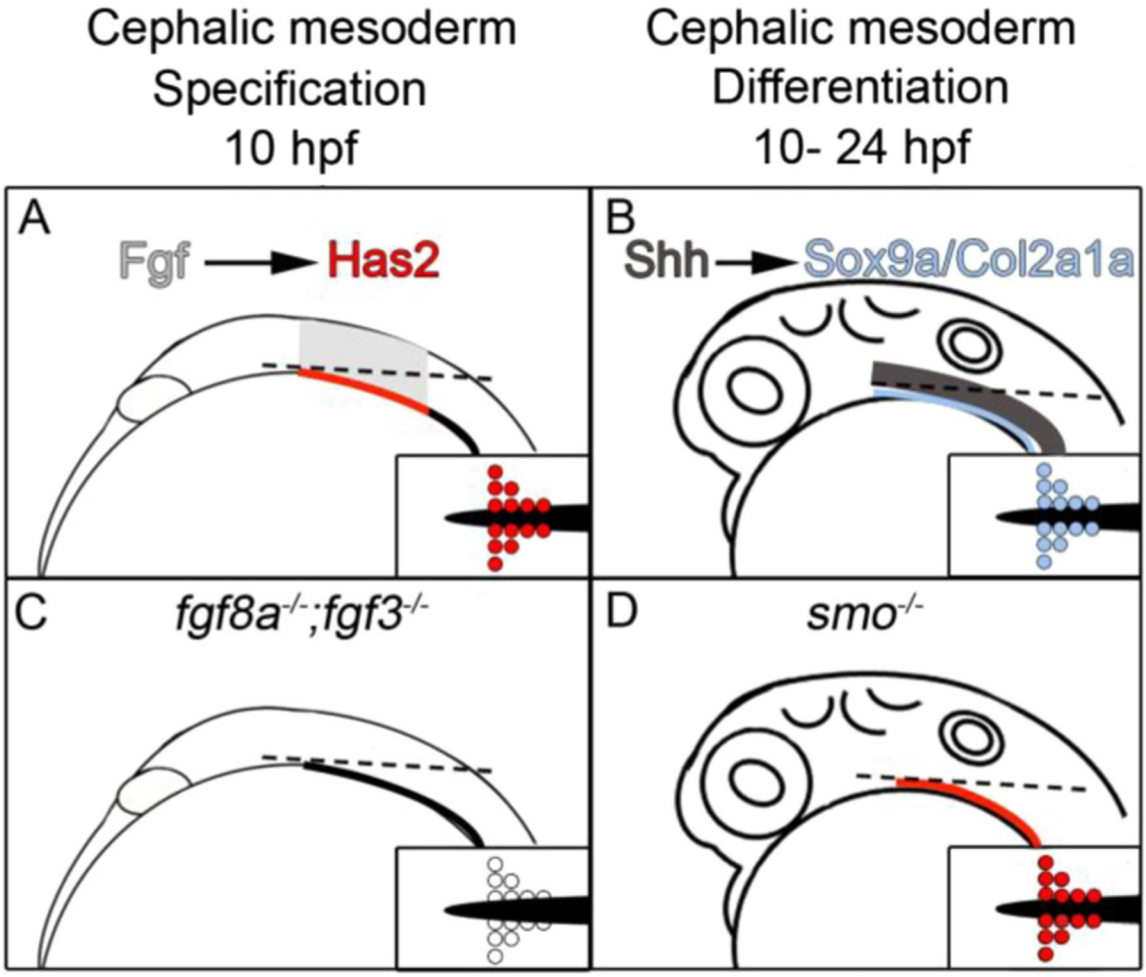

Fig. 12.

Cephalic mesoderm specification and differentiation utilizes Fgf and Hh signaling pathways. (A) During early postchordal mesoderm specification, Fgf signaling from both the overlying neuroectoderm and mesoderm is necessary for *has2* expression in mesodermal progenitors of the postchordal neurocranium. (B) During differentiation, Hh signaling from the overlying neuroectoderm promotes the expression of *sox9a* and *col2a1a* in these mesodermal cells. (C) Loss of *fgf8a* and *fgf3* results in a loss of *has2* expression in mesodermal cells, while (D) reduced Hh signaling results in loss of proper differentiation of these cells.